Environment International 202 (2025) 109684

Contents lists available at ScienceDirect

Environment International

journal homepage: www.elsevier.com/locate/envint

Full length article

Exposure to the growth promoter tylosin elicits gut microbiota disruption and metabolic imbalance in mouse model☆

Hongyuhang Ni [a,b], Jing Wang [a], Haoze Wu [b], Bill Kwan-wai Chan [a], Kaichao Chen [a], Han Wang [a,b], Edward Wai-Chi Chan [a], Fuyong Li [c], Sheng Chen [a,d,*]

[a] Department of Food Science and Nutrition, Faculty of Science, The Hong Kong Polytechnic University, Kowloon, Hong Kong Special Administrative Region
[b] Department of Infectious Diseases and Public Health, Jockey Club College of Veterinary Medicine and Life Sciences, City University of Hong Kong, Kowloon, Hong Kong Special Administrative Region
[c] Department of Animal Science and Technology, College of Animal Sciences, Zhejiang University, Hangzhou 310058, China
[d] Shenzhen Key Lab for Food Biological Safety Control, The Hong Kong Polytechnic University Shenzhen Research Institute, Shenzhen 518057, China

ARTICLE INFO

Handling Editor: Adrian Covaci

Keywords:
Tylosin
Blautia
Arachidonic acid
Metabolic dysregulation
Obesity

ABSTRACT

The environmental risk associated with the usage of the antibiotic tylosin as an animal growth promoter (AGPs) needs to be assessed because such agents are used in abundance and contamination of the environment is common, yet their effects on the physiology and gut microbiota composition of animals and humans are poorly understood. In this work, we performed metagenomic analysis and revealed that tylosin significantly disrupted the gut microbiota structure of animals, reduced species diversity, and caused the increase in the relative abundance of *Blautia* (60.95%). Enrichment of multiple contigs containing ARGs was observed, indicating that tylosin promotes antimicrobial resistance (AMR) development. Transcriptomic analyses of ileum tissues revealed perturbation in gene expression patterns suggestive of mitochondrial dysfunction and energy metabolism imbalance. These alterations might compromise nutrient absorption and utilization in the GI tract, and heighten the risk of development of obesity and non-alcoholic fatty liver disease (NAFLD). Furthermore, downregulation of immune-related gene expression was observed, indicating that tylosin caused immunosuppression and increased susceptibility to microbial infections when used over extended periods. Integrated omics analysis of the liver also showed significant disturbances in metabolism through activation of the arachidonic acid metabolism pathway, exacerbating inflammatory responses, and precipitating the occurrence of metabolic disorders such as type 2 diabetes mellitus (T2DM) and NAFLD. Our findings unveil the detrimental effects of tylosin on animal gut microbiota and metabolic functions and highlight the potential health risks to wildlife and humans when released into the environment. These findings highlight a need for cautious use of AGPs and the development of safer alternatives.

1. Introduction

Since the accidental discovery over 70 years ago that antibiotics could enhance meat production in livestock farming, their use has effectively helped cope with the food demand of the rapidly increasing human population (Evangelista et al. 2022). During the golden age of antibiotic development from the 1940 s to the 1960 s, in particular, an increasing number of sub-therapeutic antibiotics (STAs) were utilized as feed additives in the production of various types of livestock upon receiving legal approval in several European countries (Biely and March 1951; Fernández Miyakawa et al. 2024). It was reported that the amount of antibiotics used on animals was approximately twice that used in humans, and that the projected amount of antibiotic consumption for food animal production is expected to reach 105,569 tons by 2030 (Ayalew et al. 2022; Gonzalez Ronquillo and Angeles Hernandez 2017). However, the expanding livestock industry's reliance on AGPs carries significant environmental risks. For instance, 30–90% of administered veterinary antibiotics are excreted unmetabolized into animal manure

☆ This article is part of a special issue entitled: 'Food safety & Env. health' published in Environment International.

* Corresponding author at: Department of Food Science and Nutrition, Faculty of Science, The Hong Kong Polytechnic University, Kowloon, Hong Kong Special Administrative Region.
E-mail address: sheng.chen@polyu.edu.hk (S. Chen).

https://doi.org/10.1016/j.envint.2025.109684
Received 16 October 2024; Received in revised form 13 May 2025; Accepted 13 July 2025
Available online 14 July 2025

and urine, which is often directly applied to fields as a fertilizer supplement (Patyra et al. 2020; Zalewska et al. 2021). This practice introduces antibiotic residues into soils and waterways, where they exert persistent selection pressure, enriching antimicrobial resistance genes (ARGs) in environmental microbiomes (Wang et al. 2021). These ARGs can disseminate across pathogenic and environmental bacterial populations through horizontal gene transfer, accelerating the spread of resistance (Li and Zhang 2022). Furthermore, it may interact with emerging contaminants such as microplastics, forming composite pollutants that enter aquatic organisms and humans via food chains, posing long-term ecological and health risks (Dong et al. 2021; Feng et al. 2021; Founou et al. 2016).

To address AMR threats stemming from environmental contamination by AGPs, the European Union, China, and the United States have enacted regulatory policies to restrict their use (Maron et al. 2013; Wen et al. 2022). However, critical enforcement gaps persist. Ambiguous classification systems enable antibiotics approved for therapeutic purposes to be misused as growth promoters, exemplified by tylosin a macrolide accounting for 30.4% of the U.S. veterinary market (Sarmah et al. 2006). Similarly, in Thailand, tylosin is routinely added to swine feed under the guise of disease prevention, despite its unequivocal growth-promotion intent (Hallenberg et al. 2020; Kline and Pinckney 2016). Tylosin's environmental persistence is evidenced by fecal concentrations reaching 115.5 mg/kg post-administration in cattle, with residues detectable in matured manure (0.11 mg/kg) 30 days post-treatment (De Liguoro et al. 2003). Similarly, intramuscular administration of tylosin (10 mg/kg bw/day) in sheep resulted in fecal drug levels peaking at 29.7–34.3 mg/kg within 15 h (Ishikawa et al. 2018). Moreover, tylosin has been detected at concentrations ranging from 0.2 to 50 μg/L in surface waters, with its photostability extending its half-life to 200 days (Kline and Pinckney 2016; Yang et al. 2023). These residues also reduce soil microbial diversity while enriching resistance genes like *carB* and *msrc-01* and inhibiting photosynthesis and DNA repair in phytoplankton (Li et al. 2021; Sun et al. 2021). Such regulatory ambiguity, coupled with inconsistent global policies, sustains AGPs as ecological time bombs, perpetuating resistance gene reservoirs that jeopardize the ecosystem and public health.

On the other hand, the primary functions of AGPs include inhibiting microbial competitors for nutrients, preventing subclinical infections, reducing growth-inhibiting microbial metabolites, and enhancing nutrient absorption by thinning the intestinal barriers long overshadowed critical inquiries into their direct metabolic impacts on host organisms (Butaye et al. 2003). While current research predominantly attributes AGPs' growth-promoting effects to gut microbiota modulation, mounting evidence reveals that these agents may bypass microbial mediation to directly disrupt mammalian metabolic homeostasis (Brown et al. 2016; Fernández Miyakawa et al. 2024). Notably, antibiotics are intrinsically bioactive molecules with documented hepatorenal toxicity, and some studies associate their use with obesity-linked pathologies such as nonalcoholic fatty liver disease (NAFLD) and systemic insulin resistance (Mahana et al. 2016). The weight gain induced by AGPs may underlying metabolic imbalances, where rapid growth coexists with subclinical organ damage and compromised immune function.

In this study, we designed an 8-week murine feeding trial simulating high-dose tylosin regimens used in unregulated agricultural use. Through the integration of multi-omics analyses including metagenomics, metabolomics, and transcriptomics with comprehensive physiological profiling, it was systematically evaluates how tylosin disrupts gut microbiota, increases AMR, and directly alters host metabolic pathways. Our model captures the longitudinal accumulation of ARG in the gut, highlighting the potential for increase environmental dissemination through manure-amended soils. Crucially, we demonstrate that tylosin-induced weight gain correlates with antibiotic-driven direct host toxicity, which may be exacerbated by environmental drug persistence. These findings underscore the urgent need to re-evaluate AGP usage under a One Health framework, to protect the agricultural productivity and environment.

2. Materials and methods

2.1. Experimental design of the animal studies

Male ICR mice, purchased from the Labroratory Animal Research Unit (LARU) at City University of Hong Kong, were used as animal models in compliance with ethical guidelines approved by the Animal Research Ethics Subcommitee of the Univeristy (Project No: A-0744). All mice were pre-acclimatized in cages (n = 5 per cage) for one week prior to test. The mice were randomly divided into two groups to investigate the effects of oral administration of tylosin on weight gain and metabolism. The control group received *ad libitum* access to standard food and water, while the experimental group was provided with distilled water containing 0.08 mg/mL tylosin. With an average daily water intake of 6 mL per mouse and an initial body weight (~25 g), the calculated dosage reached ≤ 20 mg/kg bw/day (Bachmanov et al. 2002). This dosage was according to therapeutic levels in poultry clinical interventions and accounts for environmental bioaccumulation risks observed in livestock operations through fecal persistence (De Liguoro et al. 2003; Lee et al. 2024). Elevated dosages, consistent with antibiotic toxicity research practices, were implemented to improve the detection sensitivity of chronic effects (Luan et al. 2021). The total duration of the test was 8 weeks, feces were collected weekly and stored at −80 °C for subsequent analysis of the gut microbiota.

To monitor the phenotypic alterations in the mice, the body weight (g) was recorded every day, and the lengths (cm) of their tails and bodies (anal-to-nasal distance) were measured every week. The relative weight gain (%) and Lee's index, which can assess the body fat content and obesity in mice, were calculated according to Eqs. (1) and (2) (Hioki et al. 2010; Ni et al. 2024):

$$Relative\ weight\ gain\ (\%) = \left(\frac{Final\ body\ weight\ (g) - Initial\ body\ weight\ (g)}{Initial\ body\ weight\ (g)}\right) \times 100 \quad (1)$$

$$Lee's\ index = \frac{\sqrt[3]{Body\ weight\ (g)} \times 1000}{Naso - anal\ length\ (cm)} \quad (2)$$

Additionally, the weight of chow (g) and the volume of remaining H_2O (mL) were measured every three days to record the consumption of water and food by the mice.

After 8 weeks, the mice were euthanized, initially by blood collection from the retroorbital plexus, followed by plasma collection through standing and centrifugation, and immediately stored at −80 °C until used for biochemical and metabolite analyses. The liver and kidney tissues were weighted; a portion was fixed in a 10% formalin solution for Hematoxylin and Eosin (H&E) staining analysis. Another portion of liver and ileum tissues was washed with phosphate-buffered saline (PBS), rapidly frozen in liquid nitrogen, and stored at −80 °C for metabolite analysis or RNA extraction.

2.2. Determination of serum biomarkers

The concentrations of glucose, insulin, and lipids in the serum can effectively reflect the changes in lipid and carbohydrate metabolism induced by tylosin in mice. Initially, the levels of total cholesterol (TC), triglycerides (TG), and high-density lipoprotein (HDL) were directly measured using commercial assay kits (Stanbio Laboratory, Boerne, USA), while the content of low-density lipoprotein (LDL) was obtained using the following Eq. (3):

$$LDL\ (mg/dL) = TC\ (mg/dL) - \frac{TG\ (mg/dL)}{5} - HDL\ (mg/dL) \quad (3)$$

The insulin levels were measured using an ELISA kit (Invitrogen, Thermo Fisher Scientific, USA) according to the instructions. The glucose levels were directly determined using a commercial glucometer (GlucoSure AutoCode, ApexxBio, Taiwan).

2.3. Histopathological analysis

Kidney and liver samples were fixed overnight in a 10% neutral buffered paraformaldehyde solution at 4 °C. The fixed samples were then subjected to a standardized histopathological protocol (Cui et al. 2024). Briefly, samples underwent gradient ethanol dehydration (75%, 85%, 95%, and 100% ethanol for 1 h each) followed by xylene clearing and paraffin embedding. Tissue sections of 4 μm thickness were cut using a rotary microtome, mounted on glass slides, and subjected to sequential dehydration through a graded ethanol series (100%, 95%, 85%, 75%,) for 5 min each. Following dewaxing in xylene and rehydration, standard hematoxylin and eosin (H&E) staining was performed. Digital images were captured using an Olympus BX53 microscope at the Veterinary Diagnostic Laboratory (VDL), City University of Hong Kong.

2.4. Sample DNA extraction, library generation, and metagenomics analysis

Total bacterial DNA was initially extracted using the QIAamp® PowerFecal® DNA Kit (Qiagen, Germany) from fecal samples (n = 5 per group) following the manufacturer's instructions. The sample size is adequate for the metagenomic analysis requirement and 4R principle (Geng et al. 2025; Kiani et al. 2022). All samples were then sent to Biomarker Technologies Co., Ltd (Beijing, China) for sequencing with passing preliminary quality control for nucleic acid concentration. DNA samples were mechanically fragmented using an ultrasonicator, which generated fragments ranging from 200 to 300 bp in size. The fragments were used to construct paired-end libraries using the NEBNext® Ultra™ DNA Libraries prep kit. Subsequently, Illumina HiSeq 2500 platform (Illumina Inc., San Diego, CA, USA) was used to perform sequencing.

Fastp [v0.23.4] and Bowtie2 [v2.5.2] were used to filter raw tags and align them with the host genome sequences (*Mus musculus*, GRCm39), respectively, to remove host contamination and obtain clean reads (Chen 2023; Langmead and Salzberg 2012). MEGAHIT [v1.2.9] and QUAST [v5.2.0] were utilized for metagenomic assembly and quality assessment, respectively. MetaGeneMark [V3.26] was employed to identify coding regions, and MMseqs2 was utilized to remove sequence redundancy. Coverage thresholds and similarity were set at 90% and 95%, respectively (Gurevich et al. 2013; Li et al. 2016; Steinegger and Söding 2017). Based on the NR databases, the gene sets were annotated using Diamond (V0.9.36), with an E-value threshold of ≤ 1e-5 (Feng et al. 2022). Annotation of the abundance of antibiotic resistance genes (ARGs) was conducted by aligning sequences with the CARD database, using the RGI software (Alcock et al. 2023). Raw microbial counts were first normalized using the Trimmed Mean of M−values (TMM) method to account for sequencing depth variations (Heo et al. 2016). The α-diversity Shannon indices were analyzed using the vegan package [v2.5.6] (Liu et al. 2023a). The β-diversity analysis was conducted using PCoA based on genus- and species-level Bray-Curtis distance matrices (Dixon 2003; Litichevskiy et al. 2025). The first two principal coordinates (PCo1 and PCo2) were retained to visualize the variance structure. Different taxa across phylogenetic levels (from phylum to genus) between different time points (Week 0, Week 4, and Week 8) were identified using LEfSe analysis. Taxa were considered significant if they met both a Kruskal-Wallis rank-sum set test threshold (p-value < 0.05) and LDA effect size > 4.0 (Zou et al. 2020). PCoA and microbiome stacked charts were visualized through the OmicShare online platform (https://www.omicshare.com/tools), and Cladogram for LEfSe was analyzed and visualized using the BMKCloud platform (https://www.biocloud.net).

Binning analysis was employed to further investigate the migration of ARGs among gut microbiota strains following tylosin treatment. Specifically, MetaWRAP [v1.3] processing modules were utilized for quality control and sequence assembly (Uritskiy et al. 2018). The binning of contigs was performed using both Metaba2 [v2.11.3] and MaxBin2 methods (Kang et al. 2015; Wu et al. 2015). Within MetaWRAP, the Quant_bins and Classify_Bins modules were executed with default parameters to perform quantification and classification. Finally, Abricate [v1.0.4] was used in conjunction with the Resfinder database to identify and screen for ARGs in the binned metagenome-assembled bacterial genomes.

2.5. 16S rRNA gene sequencing analysis

To explore the dynamic changes in the gut microbiota structure during the test period, extracted fecal DNA samples from 7 time points (from Week 1 to Week 8, n = 5 per group) were also sent to Biomarker Technologies Co., Ltd for analysis using 16S rRNA sequencing. Initially, full-length 16S rRNA was amplified using universal primers (27F, AGRGTTTGATYNTGGCTCAG; 1492 R, TASGGHTACCTTGTTASGACTT) with the following PCR reaction conditions: 1 cycle at 95 °C for 5 min, followed by 30 cycles at 95 °C for 1 min, annealing at 58 °C for 1 min, and extension at 72 °C for 2 min, followed by 1 cycle at 72 °C for 10 min. The PCR products were purified, quantified, and homogenized to generate an SMRT bell library, which was sequenced on the PacBio Sequel II platform for next-generation high-throughput sequencing (Chen et al. 2022a). The output files in BAM format were then converted to CCS files using SMRT Link [v8.0.0] (Ardui et al. 2018). Specifically, barcode sequences were converted to Raw-CCS sequences using lima [v1.7.0], and Clean-CCS sequences were generated by removing primer sequences based on length with cutadapt [v1.9.1] (Martin 2011; Wang et al. 2022). DADA2 [v1.16.0] and QIIME2 [2020.6] were used for denoising and chimeric removal to produce high-quality Non-chimeric CCS sequences (Hall and Beiko 2018). Subsequently, OTUs were clustered at 97% similarity using USEARCH [v10.0.240_i86] and annotated based on the Silva database [SSU138] to obtain precise species information (Dueholm et al. 2020). The species data were visualized using stacked charts on the OmicShare online platform.

2.6. Tissue RNA extraction, library generation, and transcriptomics analysis

Total RNA was extracted from liver and ileum samples (n = 3 per group) using TRIzol reagent (Invitrogen), and initially assessed for concentration and purity using the NanoDrop™ ONE^c (Thermo Scientific). The sample size suffices for the demand of transcriptomic analysis (Wang et al. 2024). RNA samples that met quality standards were then sent to Biomarker Technologies Co., Ltd for further processing. Specifically, RNA samples were re-evaluated for purity, concentration, and integrity using the NanoDrop™ 2000c spectrophotometer and the Agilent 2100 Bioanalyzer (Agilent Technologies, USA). Only samples with an RNA Integrity Number (RIN) greater than 7.0 were used for subsequent transcriptome sequencing. The transcriptome library was prepared using the TruSeq™ RNA Sample Preparation Kit (Illumina, CA, USA), and sequencing was performed on the Illumina NovaSeq 6000 platform in PE150 mode. The resulting data were analyzed on the BMKCloud platform (https://www.biocloud.net). Trimmomatic [v0.39] was used to remove adapter-containing reads to obtain high-quality clean data (Bolger et al. 2014). Subsequently, HISAT [v2.2.1] was employed to align the sequences with the reference genome *Mus musculus* (GRCm39) to obtain mapped data (Kim et al. 2019).

The DESeq2 [v2.1.0] R package was employed to identify differential expressed genes (DEGs) between the tylosin and control groups using raw count data (Love et al. 2014). Multiple testing correction was performed using the Benjamini-Hochberg method to control FDR at 5% (Quarato et al. 2023). Genes with $|\mathrm{Log_2(fold\ change)}| \geq 1$ and adjusted

p-value (p_{adj}) < 0.05 were classified as differentially expressed (Zhang et al. 2023). Volcano plots and PCA were visualized using ggplot2 [v3.5.0] to display information on DEGs (Villanueva and Chen 2019). The first two principal coordinates (PC1 and PC2) of PCA analysis were retained to visualize the variance structure. To uncover more useful pathway information, the Kyoto Encyclopedia of Genes and Genomes (KEGG) database was also used to annotate the DEGs (Kanehisa and Goto 2000). Pathways with an adjusted p-value (p_{adj}) < 0.1 were considered significant and visualized using the Weishengxin (https://www.bioinformatics.com.cn) online platform. The protein–protein interaction (PPI) network of DEGs annotated by significant KEGG pathways was performed by the database STRING (cn.string-db.org) and visualized by Cytoscape [v3.8.0] (Cline et al. 2007; Szklarczyk et al. 2010). A high degree of connectivity in the network was obtained by using the plugin of CytoHubba (Chin et al. 2014), where the hub genes were also visualized using a heatmap on the Weishengxin online platform.

2.7. Metabolites extraction, LC-MS, and metabolomics analysis

All samples (n = 6 per group, according to the metabolomic requirements) to be tested were transported to Biomarker Technologies Co., Ltd using dry ice and initially subjected to metabolites extraction by the following procedure (Alqahtani et al. 2024): 100 μL plasma sample were mixed with 500 μL of extraction solvent (acetonitrile: methanol = 1:1), and vortexed for 30 s, and then sonicated in an ice water bath for 10 min. For the liver sample, a 50 mg tissue sample was mixed with 1000 μL of extraction solvent (methanol: acetonitrile: H_2O = 2:2:1) containing internal standards. The mixture was combined with steel beads and subjected to grinding at 45 HZ for 10 min, followed by sonication in an ice-cold water bath for an extra 10 min. All samples were then left to stand at −20 °C for 1 h, and centrifuged at 4°C and 12,000 rpm for 15 min. The supernatant was transferred to a new tube, and metabolites were extracted by drying in a vacuum concentrator. The extracts were then reconstituted in 160 μL of extraction solvent (acetonitrile: H_2O = 1:1), vortexed for 30 s, and sonicated in an ice water bath for 10 min. Lastly, 120 μL of supernatant was transferred to a vial after centrifuging at 4°C and 12,000 rpm for 15 min, and 10 μL of the sample was injected into the machine for analysis. Untargeted metabolomic analysis was performed via liquid chromatography coupled to tandem mass spectrometry (LC-MS) (Waters, UPLC; Thermo, QExactive) equipped with a chromatography column.

The MS data was acquired in both the positive and negative ion modes. The raw MS data were then aligned to the peaks using the Progenesis QI software (Zhang et al. 2016). Each fragment was identified by analyzing the retention and m/z data, with metabolites annotation and data normalization performed using the XCMS R package (Smith et al. 2006). The annotated data were matched against the KEGG and HMDB databases for metabolite identity confirmation. The PCA was performed to assess the quality and reproducibility of metabolomic data in all groups. The first two principal components (PC1 and PC2), which captured the majority of the variance, were retained to visualize the global variance structure. OPLS-DA model was performed to assess the differences in metabolite profiles between control and tylosin groups, and the Variable Importance in Projection (VIP) values were calculated through multiple cross-validation (Huang et al. 2018). The model performance was evaluated using R^2 (explained variance of X/Y matrices) and Q^2 (predicated capacity via cross-validation) (Rushing et al. 2022). The criteria for screening differential metabolites were set as $|Log_2(\text{fold change})| > 1$, univariate statistical p-value < 0.05, and VIP > 1 (Li et al. 2023). Volcano plots were utilized to visualize the differences, which were displayed on the Weishengxin online platform. Additionally, the differential metabolites annotated by the KEGG database were used to explore and elucidate information on related metabolic pathways.

2.8. Integration of transcriptome and metabolomic data

To uncover the key roles specifically involved in the liver tissue response to tylosin intervention, transcriptomic and metabolomic data were integrated based on annotations from the KEGG pathway. Specifically, overlap KEGG pathways annotated by DEGs and differential metabolites were summarized initially using a Venn diagram (Venny 2.0.2, available at bioinfogp.cnb.csic.es/tools/venny/index2.0.2.html). Subsequently, Pearson correlation coefficients that depict the relationship between the specific metabolites and the corresponding genes were analyzed based on the selected pathways, and the results were visualized using a correlation network through the Weishengxin online platform.

2.9. Statistical analysis

The experimental characterization data are expressed as the mean ± SEM (n = 5). The degree of significance in the difference between the treatment and control groups was visualized and analyzed by a two-tailed unpaired Student's t-test using GraphPad Prism software version 10.2.3. A two-tailed p-value < 0.05 was considered statistically significant. Significance levels are indicated as follows: $^{\#}p < 0.1$, $^{*}p < 0.05$, $^{**}p < 0.01$, $^{***}p < 0.001$, and $^{****}p < 0.0001$. Bioinformatics analysis and visualization were conducted using the following online platforms: OmicShare (https://www.omicshare.com/tools), BMKCloud (https://www.biocloud.net), and Weishengxin (https://www.bioinformatics.com.cn).

3. Results

3.1. Tylosin-induced metabolic dysregulation and insulin resistance

Throughout the experimental period (Week 1 through Week 8), antibiotic intervention resulted in higher body weights when compared to the control group. The relative weight gain (%) in the tylosin group (45.69 ± 0.97%), was higher than the 39.85 ± 1.22% observed in the control group (Fig. 1**a**). Simultaneously, Lee's index, which indicates the degree of obesity, also reached 395.88 ± 4.40 after 8 weeks of antibiotic exposure, representing an increase of 8.39% from the baseline; in comparison, there was virtually no alteration in the control group (Fig. 1**b**). Consistently, the amount of water consumed and food intake in mice fed with tylosin were higher than those in the control group in Week 1 and Week 2, respectively, (Fig. 1**c-d**). This observation suggests that the intake of antibiotics altered the appetite of the mice, resulting in increased food consumption and higher body weight. However, our observation indicated that the rapid weight gain induced by tylosin was due to the accumulation of adipose tissue in different parts of the body, resulting in an obese state that critically impacts the metabolic profile of circulating fatty acids and glucose balance, such events in turn result in metabolic dysregulation and increased risk of disease onset. Our findings confirm that tylosin intake resulted in as much as 28% reduction in blood glucose levels and an elevation in insulin concentration by 1.90-fold (Fig. 1**e-f**), such changes infer the onset of insulin resistance in the host. As expected, alterations in the plasma lipid spectrum were observed. Such changes, which included elevated concentrations of TC, TG, and LDL, and a decrease in HDL levels (Fig. 1**g** and Fig. S1), are consistent with the metabolic perturbations known to be associated with obesity. Histological analysis was also employed to assess the effects of tylosin on visceral organs. The results revealed nuclear pyknosis in liver cells accompanied by inflammatory cell infiltration, and a notable enlargement of the medullary spaces in the kidneys, indicating mild tissue damage (Fig. S2a). The relative weight of organs was also found to have increased when compared to the controls, suggesting the possibility of the development of non-alcoholic fatty liver disease (NAFLD) (Fig. S2b-c). These findings demonstrate that tylosin intervention induces profound metabolic disturbances, resulting in insulin resistance, a hallmark of type 2 diabetes (T2DM), early onset of NAFLD, as well as a

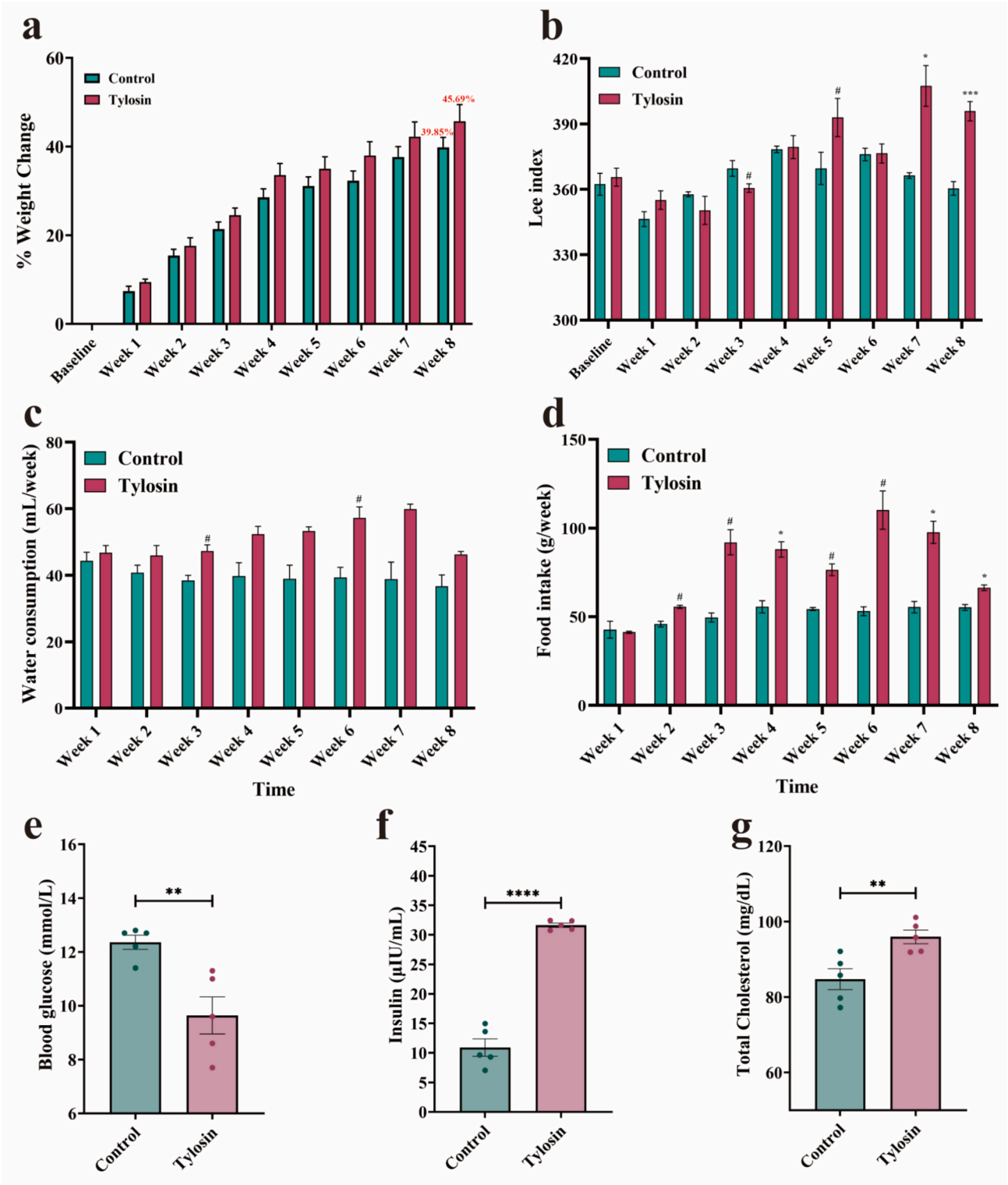

Fig. 1. Effects of tylosin on physiological and metabolic parameters in mice over an 8-weeks treatment period. (a) Relative body weight gain (%), (b) Lee's obesity index, (c) Water consumption, and (d) Food intake recorded throughout the 8-weeks intervention period; (e) Blood glucose concentration, (f) Insulin levels, and (g) Total cholesterol levels in the plasma of two groups assessed after 8 weeks of treatment. The data are shown as mean ± SEM (n = 5). Statistical significance was determined using an unpaired two-tailed Student's *t*-test. Significance was set as $^{\#}p < 0.1$, $^{*}p < 0.05$, $^{**}p < 0.01$, $^{***}p < 0.001$, and $^{****}p < 0.0001$.

certain degree of tissue damage.

3.2. Impact of tylosin on gut microbiome and ARGs migration

Results of α-diversity analysis showed that the Shannon diversity index at Week 4 and Week 8 was significantly lower than the baseline level, indicating a reduction in evenness (Fig. 2**a**). The β-diversity, represented by genus- and species-PCoA analysis, exhibited substantial differences in microbial community structure across the experimental period, reflecting profound disruption of the gut microbiota structure

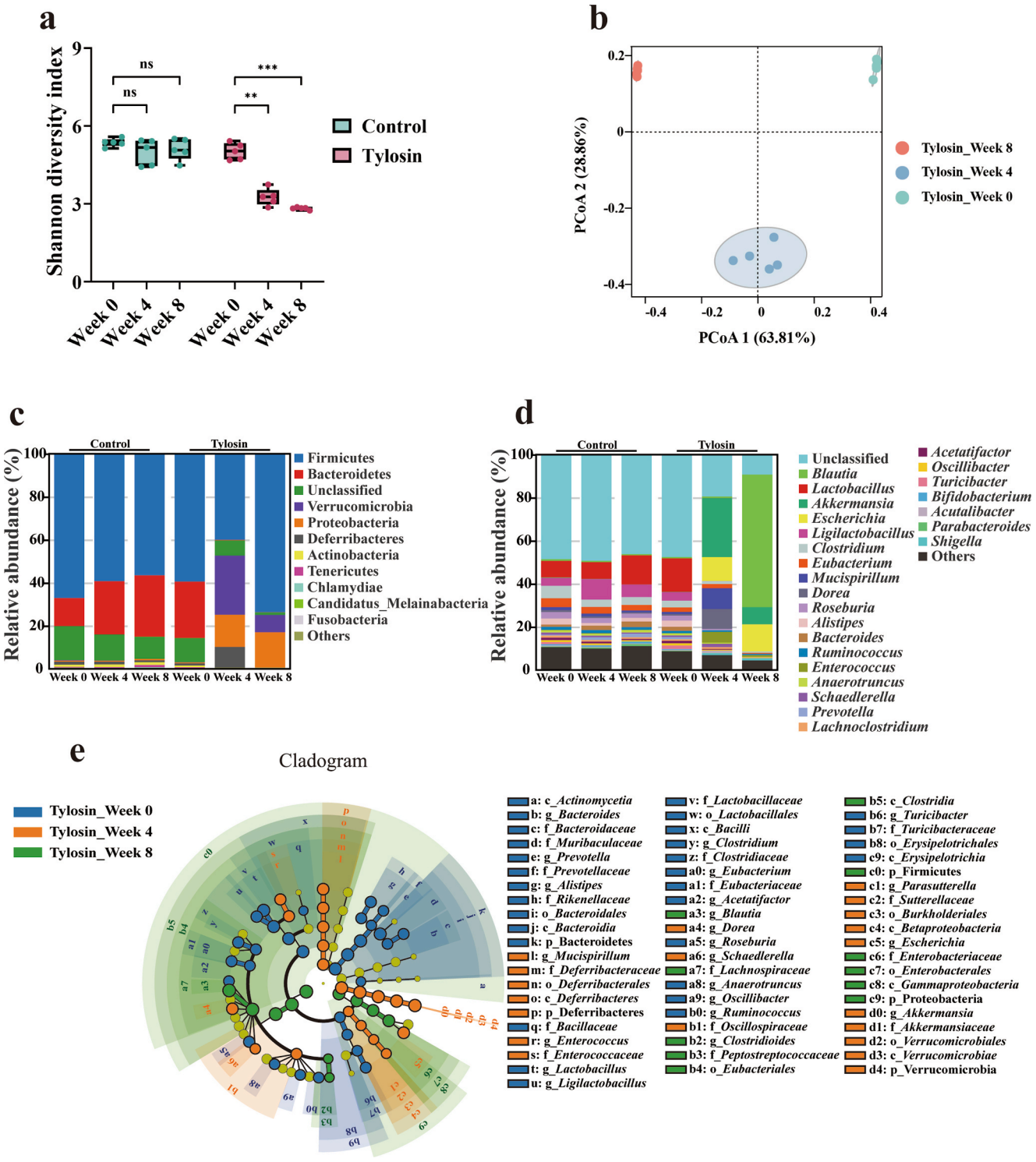

Fig. 2. Effects of tylosin on gut microbiota composition of mice determined at different time points of the treatment process. (a) Shannon index of α-diversity, (b) PCoA plots of β-diversity at the genus level in the tylosin group (PCo1 = 63.81%, PCo2 = 28.86%), (c) Relative abundance of gut microbes at the phylum level, (d) Relative abundance of gut microbes at the genus level, and (e) Circular cladogram generated by LEfSe comparison analysis (LDA score > 4) of gut microbiota at the phylum and genus levels. The data are shown as mean ± SEM (n = 5). Statistical significance was determined using an unpaired two-tailed Student's *t*-test. Significance was set as $^{\#}p < 0.1$, $^{*}p < 0.05$, $^{**}p < 0.01$, $^{***}p < 0.001$, and $^{****}p < 0.0001$.

(Fig. 2**b** and Fig. S3a).

Annotations from the Nr database provided a more detailed presentation of changes in the microbial community composition. While there were no significant changes in the control group at all levels throughout the experiment, distinct shifts in composition were observed at all 3 major time points following tylosin treatment. Specifically, at the phylum level, the relative abundance of the dominant Firmicutes decreased from 59.44% at baseline to 40.03% at Week 4, then rose to 73.69% by Week 8. Concurrently, the abundance of Bacteroidetes dropped by 5 orders of magnitude from an initial 26.18%, while Proteobacteria increased from 0.42% to 14.94% at Week 4 and remained elevated at 16.48% at the end of the study (Fig. 2**c**). It is noteworthy that

the Firmicutes/Bacteroidetes (F/B) ratio in the tylosin group increased during the process of drug intervention (Fig. S3b). At the genus level, the microbial composition became simplified upon intervention with tylosin, with most taxa being significantly reduced, including the probiotic *Lactobacillus* strains, which decreased from an initial level of 15.57% to undetectable levels (Fig. 2**d**). Notably, the relative abundance of *Akkermansia* increased from 0.13% to 27.53% before dropping to 8.03%; the abundance of *Escherichia* rose continuously to 12.50% during the 8 weeks treatment period. At the species level, *Akkermansia muciniphila* and *Escherichia coli* were identified as the primary contributors to these changes (Fig. S3c). Interestingly, the abundance of *Blautia* surged from an initial 0.61% to 61.56% throughout the study, with *Blautia producta*

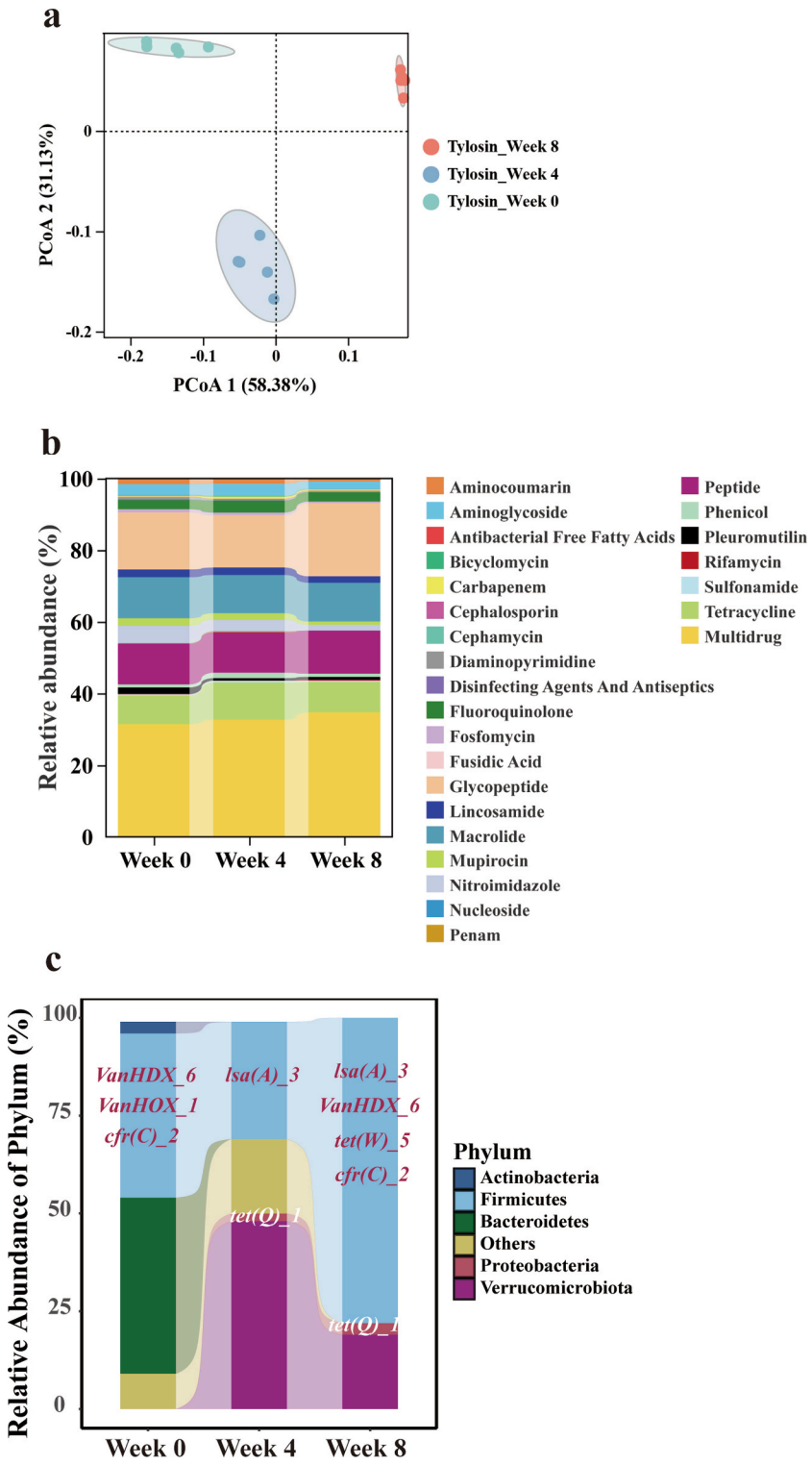

Fig. 3. Analysis of variation in antibiotic resistance genes (ARGs) profile in the gut microbiota following tylosin treatment. (a) PCoA analysis of the community based on ARGs annotated using the CARD database (PCo1 = 58.38%, PCo2 = 31.13%, n = 5), (b) Relative abundance of ARGs that encode phenotypic resistance to different classes of antibiotics, and (c) Stacked bar chart showing the relative abundance of gut microbiota at the phylum level, with data derived from metagenomic binning analysis. Annotations include the shift of ARGs profiles across key different time points.

increasing by 11.62%, the rest being unclassified species. Further analysis by 16S rRNA sequencing revealed dynamic shifts in bacterial composition from Weeks 1–7 (Fig. S3d). The gut microbiota structure was profoundly affected just one week after tylosin administration, with *Akkermansia* constituting over 25.04% and *Escherichia* spiking to 56.00%, the abundance of these species gradually decreased until a resurgence in Week 7. *Blautia* became the dominant strain by Week 7, constituting 50.00% of the microbiome, LEfSe analysis based on LDA score also supported these findings, highlighting *Akkermansia* and *Blautia* as the most differentially enriched genera at Weeks 4 and 8, respectively (Fig. 2**e** and Fig. S4). These results indicate that tylosin intervention causes rapid and significant disruption to the gut microbiome, with continual shifts in the microbial structure being observed throughout the study period; implications of such changes for host metabolism need to be further studied.

Prolonged antibiotic intervention not only disrupts microbial communities in the intestine but also causes a shift in ARGs profiles, posing a risk of expansion of antibiotic-resistant bacterial population in the gut microbiota of animal hosts as well as in different environmental niches. We next analyzed the degree of enrichment of ARGs in the gut microbiota of the test mice using annotations from the CARD database. PCoA showed that the ARGs patterns recorded at the 3 key time points were distinct and non-overlapping (Fig. 3**a**). Based on antibiotic resistance gene categories, we observed an increase in the abundance of genes that encode resistance to glycopeptide antibiotics from 15.96% at Week 0 to 20.47% by Week 8 (Fig. 3**b**). Subsequently, we found that all ARGs within this category were vancomycin resistance genes (Table S1). To investigate the migration of ARGs among specific intestinal microbial taxa, we employed metagenomic binning tools to assemble the genomic information of each species individually. The results indicated that post-tylosin treatment, numerous resistance gene contigs, including *vanHDX_6*, *tet(W)_5*, and *crf(C)_2*, were preferentially enriched in the genome of *Blautia* (Fig. 3**c** and Table S1). Therefore, tylosin not only affects the structural integrity of the gut microbiome but also profoundly alters the distribution and transmission of functional genes therein, resulting in the concentration of resistance genes in the enriched bacterial species.

3.3. Tylosin-induced downregulation of immune function in the GI tract

In addition to an assessment of intervention and disruption of the gut microbiota, we further explored the effects of tylosin on gastrointestinal (GI) tract tissues using transcriptomic analysis approaches. Initially, PCA demonstrated significant differences in the ileum gene expression profiles between the test and control groups (Fig. 4**a**). The volcano plot further revealed regulatory changes in the genes, specifically identifying 285 and 721 genes that exhibited significant upregulation or downregulation, respectively ($|\mathrm{Log_2}(\text{fold change})| > 1.0$, $p_{adj} < 0.05$) (Fig. 4**b** and Table S2). Using the KEGG database for enrichment annotation of these DEGs, several pathways related to energy metabolism and associated disease development were found to be significantly activated ($p_{adj} < 0.1$), including “Oxidative phosphorylation”, “Arachidonic acid metabolism”, “Diabetic cardiomyopathy”, and “Non-alcoholic fatty liver diseases” (Fig. 4**c** and Table S3). In contrast, the downregulated pathways are mainly associated with immune regulation and inflammatory response, such as “Cytokine-cytokine receptor interaction”, “Th1 and Th2 cell differentiation”, “Th17 cell differentiation” and “TNF signaling pathway”. Besides, the “Intestinal immune network for IgA production” pathway, which plays a role in the differentiation of intestinal immune cells, also exhibited significant alterations. These observations show that tylosin intervention has a significant negative impact on the GI tract, including disruptions in metabolic functions and potential suppression of the host immune response.

Following the annotation of significant KEGG pathways for DEGs, we constructed a PPI regulatory network to identify the most crucial Hub genes within the entire expression profile by utilizing the Cytoscape software (Fig. 4**d** and Fig. S5). The results indicated that the top 10 Hug genes were all downregulated and associated with the toxic response and regulation of the immune system, including genes such as *Gzma*, *FASL*, *Ccl5*, and *ITGAM*. Downregulation of these genes may compromise the immune response to bacterial infections.

3.4. Tylosin-induced metabolic dysfunction in liver

Transcriptomic analysis indicated that there was indeed a shift in the hepatic transcriptional profile of the test mice (Fig. 4**e**), with 265 and 372 genes exhibiting significantly upregulated and downregulated expression levels, respectively ($|\mathrm{Log_2}(\text{fold change})| > 1.0$, $p_{adj} < 0.05$) (Fig. 4**f** and Table S4). Pathway enrichment analysis via KEGG annotations revealed upregulation in the expression of genes in the pathways involved in metabolism and inflammation, such as “Arachidonic acid metabolism” as well as “Circadian rhythm” ($p_{adj} < 0.1$); conversely, expression of genes in the pathways responsible for drug metabolism and metabolism of glutathione were downregulated (Fig. 4**g** and Table S5). Subsequently, a PPI regulatory network was also constructed to identify Hub genes in the differentially expressed metabolic pathways (top-10) (Fig. 4**h** and Fig. S6). The results indicated that these key genes were predominantly downregulated, and are associated with cell cycle regulation and division; such genes include *Chek1*, *Ccne1*, *Cdc20*, and *Bub1b*. Based on the above findings, we hypothesize that tylosin, as a pharmaceutical agent, not only affects the metabolic functions of the host but also directly inflicts damage to the liver tissue with potentially dire consequences. To further investigate the hepatotoxic effects and metabolic disturbances induced by tylosin, we employed an untargeted metabolomics approach to verify specific metabolic alterations. PCA depicted significant differences between the liver metabolomic profiles of the tylosin-treated mice and the control (Fig. 5**a** and Fig. S7a-b). Specifically, when compared to the control group, there were significant increases and decreases in the abundance of 119 and 186 metabolites, respectively ($|\mathrm{Log_2}(\text{fold change})| > 1$, p-value < 0.05, and VIP > 1) (Fig. 5**b** and Table S6). KEGG annotation showed that the pathways in which the upregulated metabolites were generated were related to cancer and metabolic regulation, including “Prostate cancer”, “Arachidonic acid metabolism” and “AMPK signaling pathways”. The downregulated pathways were primarily associated with lipid metabolism, such as “Steroid biosynthesis” and “Carbohydrate digestion and absorption” (Fig. 5**e** and Table S7). These findings were consistent with the transcriptomic data, confirming that hepatic metabolic functions were impaired and that tylosin treatment is detrimental to the overall health of the host.

Interestingly, significant differences were also observed in the plasma metabolomic profiles (Fig. 5**c** and Fig. S7c-d), with 117 and 119 metabolites exhibiting significant increases and decreases in abundance levels, respectively ($|\mathrm{Log_2}(\text{fold change})| > 1$, p-value < 0.05, and VIP > 1) (Fig. 5**d** and Table S8). Upon comparison with the KEGG database, the upregulated pathways in plasma were related to endocrine and physiological metabolism, notably those involved in the onset of insulin resistance; such finding was consistent with the observed changes in blood glucose and insulin levels. On the other hand, the downregulated pathways involved sugar and carbohydrate metabolism, including galactose metabolism and carbohydrate digestion and absorption (Table S9). These results therefore further reveal the liver damage and metabolic abnormalities induced by tylosin intervention. The impact of changes in metabolite profiles may be transmitted to other organs through the circulatory system, potentially affecting multiple physiological functions and precipitating the early onset of metabolic health diseases such as T2DM and NAFLD. These findings indicate that the weight gain that occurs during tylosin treatment is the result of exacerbation of weight imbalance in the host as a result of extensive disruption of the physiological and metabolic functions of the host.

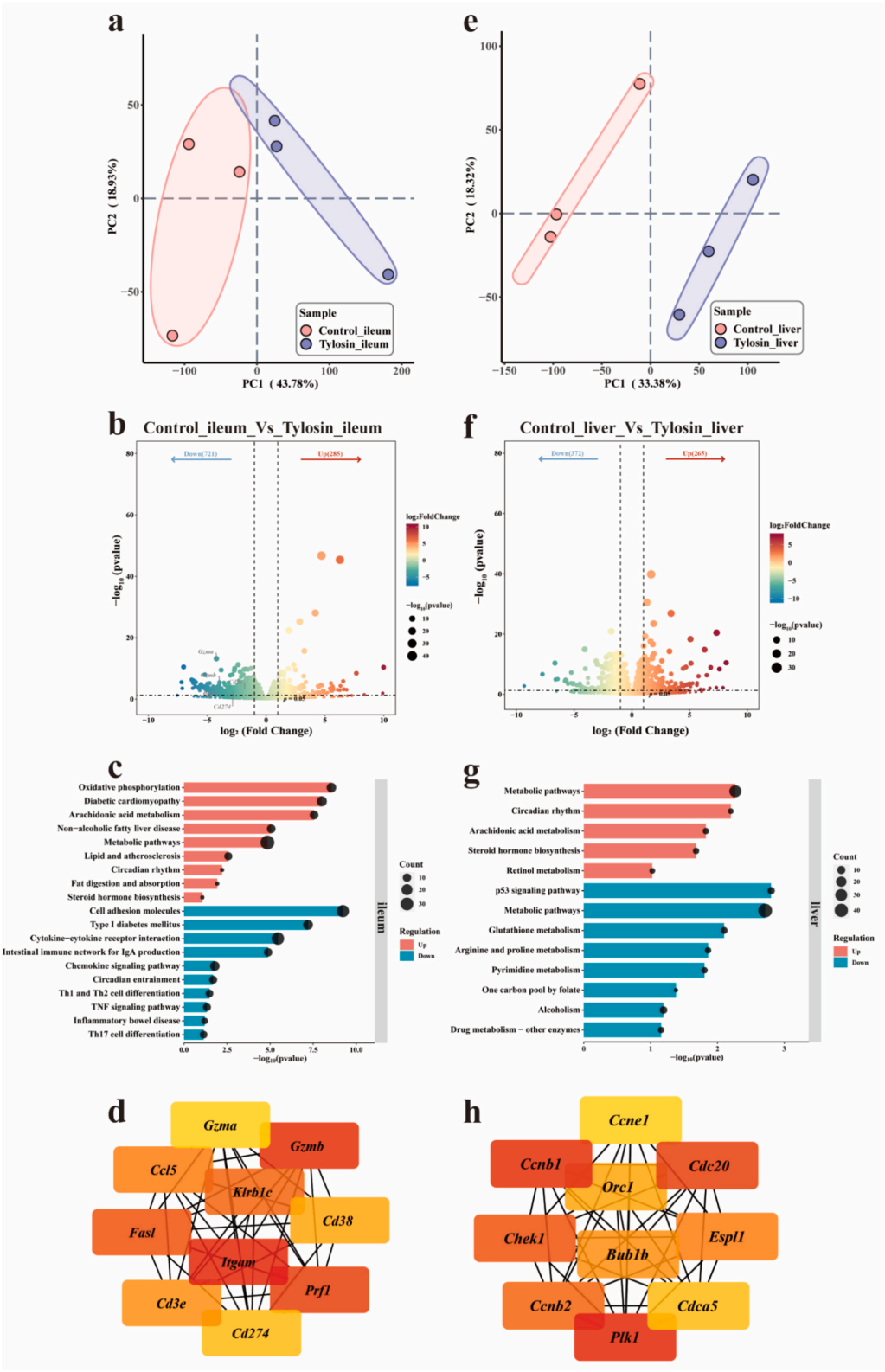

Fig. 4. RNA-Seq analysis of ileum and liver tissues of mice subjected to tylosin treatment. (a)&(e) The principal components analysis (PCA) of the transcriptome data (a: PC1 = 43.78%, PC2 = 18.93%; e: PC1 = 33.38%, PC2 = 18.32%, n = 3), (b)&(f) Volcano plots for DEGs, (c)&(g) Representative KEGG pathways enrichment of up- and down-regulated DEGs, and (d)&(h) The PPI network Top-10 hub DEGs identified from significant KEGG pathways, constructed using the STRING online database and presented by using the Cytoscape software.

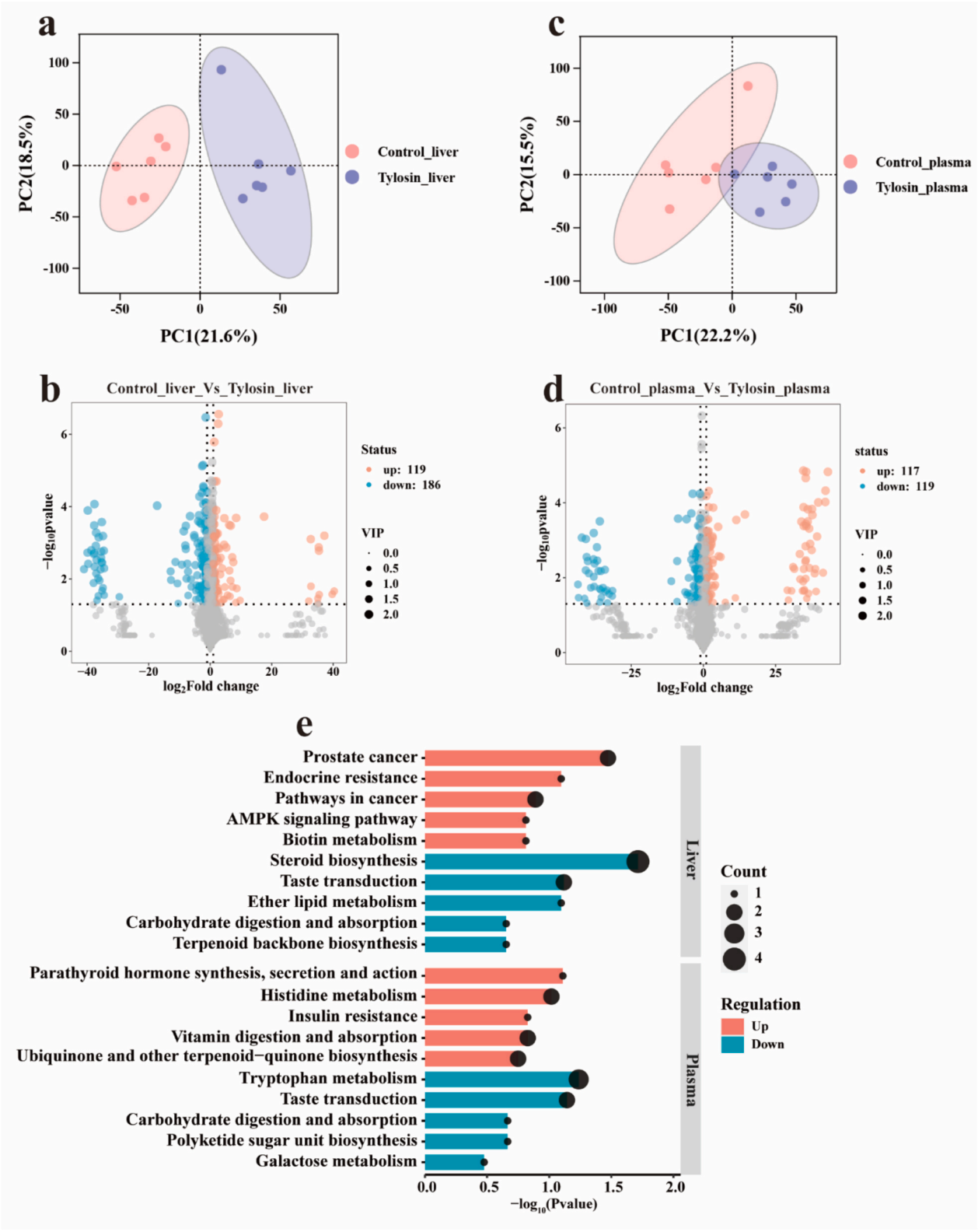

Fig. 5. Alteration of metabolite profiles in liver and plasma samples of mice subjected to tylosin treatment. (a)&(c) The principal components analysis (PCA) of the metabolomic data (a: PC1 = 21.6%, PC2 = 18.5%; c: PC1 = 22.2%, PC2 = 15.5%, n = 6), (b)&(d) Volcano plots for differential metabolite profiles recorded in control and tylosin groups, and (e) KEGG pathways enrichment of the top-5 up- and down-regulated pathways involved in generation of metabolites whose levels in liver and plasma were found to be significantly different when the two groups were compared.

3.5. Key metabolites identified from integrated omics analysis in liver

Following the observation that intervention with tylosin precipitates metabolic dysregulation and subsequent progression of health-related disorders in the host, we pursued an integrated analysis of transcriptomic and metabolomic data to screen for potential key metabolites that drive the metabolic imbalance. Initially, by employing Venn diagrams, we pinpointed 3 overlapping significant KEGG pathways annotated by both DEGs and differential metabolites (Fig. 6**a-b**). Subsequent correlation analysis using Pearson's coefficient revealed strong positive correlations between the abundance of metabolites and the related gene counts in the "Arachidonic acid metabolism" and "Steroid hormone biosynthesis" pathways, whereas the "Prostate cancer" pathway exhibited a negative correlation, with all coefficients surpassing 0.5 after normalization (Fig. 6**c**). Furthermore, the pathways that exhibit positive correlations are related to inflammation and physiological metabolism. Notably, DEGs associated with arachidonic acid metabolism, such as *Cyp2c37*, *Cyp2c50*, and *Cyp2c52*, are part of the cytochrome P450 family, which is linked to drug metabolism in the liver. Consequently, the metabolite leukotriene A4 (LTA4) appears to stand out in this analysis and is likely a pivotal agent that mediates pathogenic liver damage and metabolic disturbances. Being an inflammatory mediator, LTA4 is known to contribute to the suppression of host immune function. Therefore, LTA4 emerges as a potential major factor in the disruption of host physiological metabolism following tylosin intervention.

4. Discussion

AGPs have been regarded as beneficial to livestock farming by preventing diseases and enhancing the growth rate of animals (Pokharel et al. 2020). However, the potential health risks associated with prolonged usage of these agents remain unknown. This is an important issue as AGPs are used in abundance and environmental contamination is common (Yopasá-Arenas and Fostier 2018). If exposure to AGPs is proven to be able to cause chronic illnesses in humans and animals, it would be scientifically justified to prioritize phased restrictions on their agriculture applications and adopt evidence-based mitigation frameworks to reduce the environmental dispersion of these bioactive agents. In this work, we have generated sufficient evidence which shows that weight gain in animals induced by tylosin, a representative AGP, comes at the cost of animal health and welfare. Importantly, multiple physiological and metabolic defects were observable in animals treated with tylosin for as short as eight weeks. It is likely that antibiotic residues that

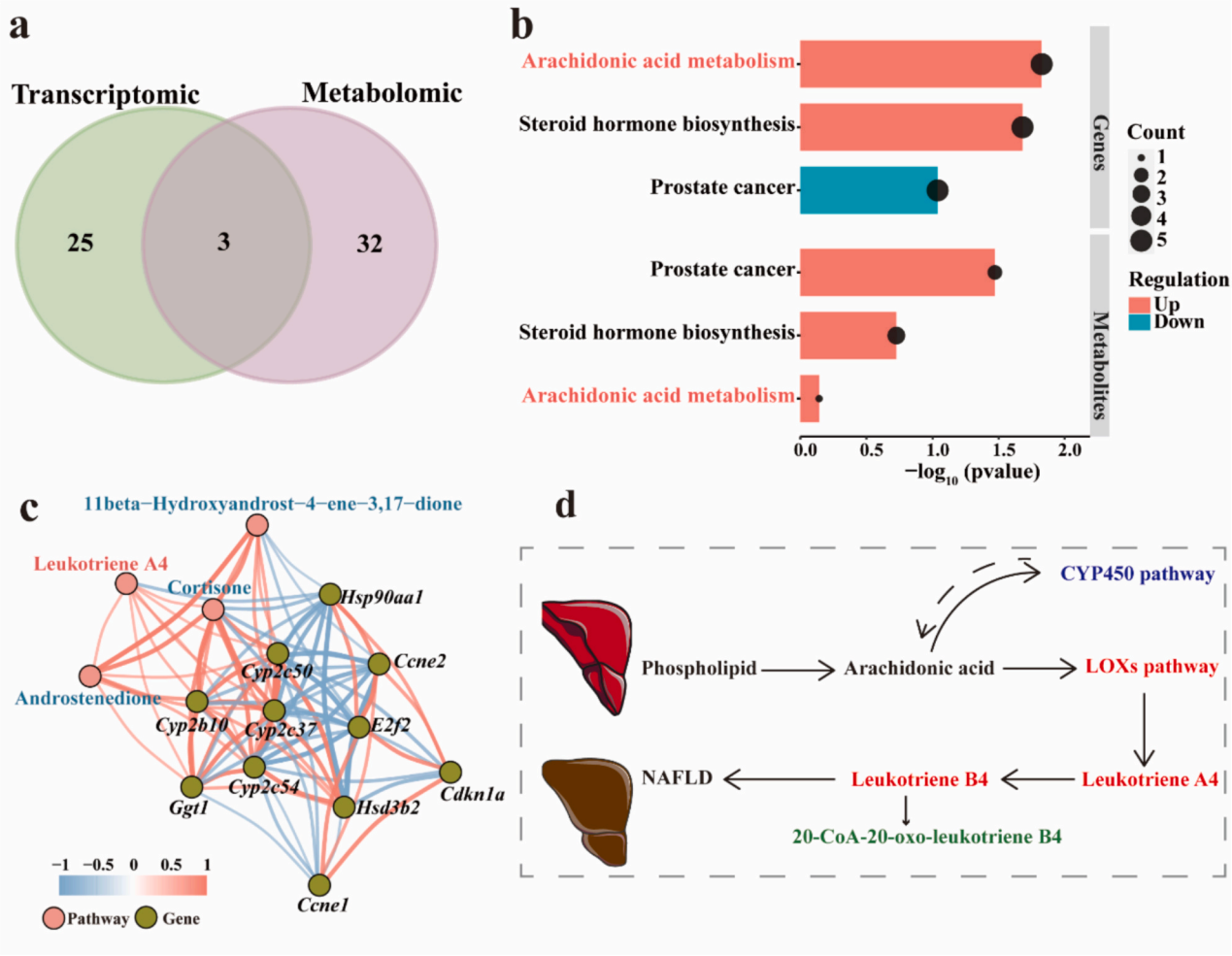

Fig. 6. Analysis of degree of correlation between transcriptome and metabolome of liver tissue collected in tylosin-treated mice. (a) Venn diagram summarizing the overlapping KEGG pathways annotated by DEGs and metabolites of significantly different levels when control and tylosin-treated groups were compared, (b) Degree of significance of the overlapping KEGG pathways, pathways with notable changes in both DEGs and differentially produced metabolites in the tylosin and control groups are highlighted, (c) Correlation network plots of representative KEGG pathways illustrating the relationship between DEGs and differentially produced metabolites based on Pearson coefficients, and (d) Tylosin-mediated hepatic damage, parts of the figure were drawn using pictures from Servier Medical Art (https://smart.servier.com/).

remain in food samples pose similar health risks to human, Hence environmental contamination with AGPs such as tylosin is of great concern.

In this study, we showed that tylosin significantly altered the appetite of male mice and caused a significant increase in relative body weight gain (45.69%) when compared to the control group. Assessment by Lee's index, however, indicated that this rapid weight gain was actually manifested in the form of obesity, rather than a healthy and natural growth phenomenon. Notably, male mice were selected due to their increased susceptibility to diet-induced weight gain and comparatively reduced gut microbiota diversity relative to females (Casimiro et al. 2021; Zhu et al. 2023). Several previous studies showed that early antibiotic treatment in infants greatly increased the likelihood of becoming overweight/obese; similar results have also been observed in animal models (Klancic et al. 2020; Vallianou et al. 2021). Treatment with AGPs last much longer and hence the effects on animals are expected to be more significant and long-lasting. It is also known that blood lipid metabolism can be disrupted by antibiotics, leading to the onset of cardiovascular diseases such as atherosclerosis (Kappel et al. 2020). Our results consistently revealed elevated levels of TC, TG, and HDL in plasma, indicating that the animal host has entered a hyperlipidemic physiological state, which may predispose further development of other metabolic diseases; the observation of liver tissue damage in our study supports this hypothesis. As a vital metabolic organ, the liver plays a crucial role in energy metabolism, drug detoxification and immune functions (Peiseler et al. 2022). This study illustrated that tylosin intervention resulted in pathological change in the liver of the test mice, and an increase in the organ weight ratio, indicating early onset of NAFLD. If not treated timely, this condition could lead to impairment of liver functions and other metabolic processes (Tilg et al. 2021). On the other hand, the liver is also a key organ that regulates blood sugar levels. In obese patients, an imbalance of blood sugar and insulin levels can trigger the onset of T2DM and exacerbate abnormalities in fat and sugar metabolism, setting off a vicious cycle (Kaufman et al. 2020; Rachdaoui 2020). In our study, although blood glucose levels were only slightly reduced, the content of insulin was abnormally elevated (1.90 times), indicating potential development of insulin resistance and signs of early symptoms of T2DM. A previous clinical cohort study indicated that prolonged use of antibiotics could increase the risk of developing T2DM in women (Yuan et al. 2020). Therefore, if exposure to tylosin continues, pancreatic β-cell functions would likely progress to exhaustion, leading to rapid increase in blood glucose levels and deterioration of the overall health of the animal host. All in all, our data confirms that the weight gain induced by the long-term feeding of tylosin is negative and unhealthy, causing significant damage to the liver of the test animal and development of serious metabolic diseases such as NAFLD and T2DM.

The prevailing view holds that the growth-promoting mechanisms of antibiotics are primarily based on their effects on the gut microbiota, such as inhibiting the growth of gut microbes that compete with the host for nutrients, suppressing sub-clinical microbial infections, and reducing microbial metabolites in the gut that are unfavorable for growth (Rahman et al. 2022). Although these effects appear to be beneficial, it is important not to overlook the fact that antibiotics are major disruptors of the gut microbiota. Administration of antibiotics frequently results in numerous detrimental effects, including diminished diversity of gut microbiota characterized by a decrease in the population size of probiotic strains, induction of antibiotic resistance, and alteration of the metabolic landscape of the gut, notably the production of bile acids and SCFAs (Gao et al. 2019; Ramirez et al. 2020). It was reported that tylosin administration at the Theoretical Maximum Daily Intake (TMDI) level (0.047 mg/kg) induced obesity and gut microbiota disruption in mice under high-fat diet conditions, with no remarkable weight changes observed in standard dietary regiments.(Chen et al. 2022b). The elevation in primary bile acid levels may exacerbate disturbances in gut microbiota through their inherent antimicrobial properties (Tian et al. 2020). Importantly, this investigation did not address the horizontal transfer of antibiotic resistance or virulence genes within microbial communities or systemic metabolic perturbations in hosts beyond adiposity. We assessed the impact of tylosin on the structure and functional genes of gut microbiota to determine the nature of damage this drug may inflict on animal health at a higher concentration in this study. Initially, the data of α-diversity and β-diversity in this study confirmed severe disruption of the gut microbiota structure and a significant reduction in evenness. Meta-analysis spanning data of strains collected in the period 1946–2019 indicated that nearly all common antibiotics cause a reduction in bacterial diversity and a decrease in the abundance of probiotic strains, with effects lasting over one year (Zimmermann and Curtis 2019). Furthermore, as a macrolide antibiotic targeting the 50S ribosomal subunit, tylosin exhibits heightened activity against Gram-positive bacteria (Liu and Douthwaite 2002). This mechanistic specificity results in selective suppression of probiotic taxa such as *Bifidobacterium* and *Lactobacillus*, ultimately driving microbial community homogenization and loss of diversity (Powell et al. 2021). Our data are consistent with these findings and show that tylosin intervention reduced the abundance of *Lactobacillus* to undetectable levels, but caused as much as a 12% increase in the abundance of *E. coli*. In animal models, *Lactobacillus* has been proven to antagonize obesity; representative examples include *Lactobacillus rhamnosus* GG (LGG), which can improve leptin resistance caused by a high-fat diet, and *Lactobacillus reuteri* J1 (*L. reuteri* J1), which ameliorates dyslipidemia and reshapes adipose tissue by inhibiting the FXR signaling pathway (Cheng and Liu 2020; Zhang et al. 2022). Hence, the reduction in abundance of probiotic strains is associated with an increased risk of obesity. On the other hand, *E. coli* abundance is typically upregulated in obese and overweight individuals, as overgrowth of this strain may disrupt physiological functions of the gut, affecting lipid and carbohydrate metabolism and inducing development of metabolic diseases (Geng et al. 2022). The F/B ratio was also found to be elevated several hundredfold after 8 weeks; this feature, which is consistent with the obesity characteristics, may be attributed to the ability of Firmicutes to enhance metabolism and fermentation of carbohydrates and lipids (Stojanov et al. 2020). In addition, the significant increase in the abundance of *Blautia* (60.95%) is of great concern. Current studies consider *Blautia* a potential probiotic strain which may prevent occurrence of metabolic and inflammatory diseases, and that this strain is less commonly found in diabetic/obese individuals; this theory therefore appears to contradict our findings (Liu et al. 2021b). However, Chanda et al. suggest that a shift in *Blautia* abundance in obese individuals might either improve or exacerbate obesity, depending on the differences of specific strains (Chanda et al. 2024). Our results at least suggest a strong correlation between *Blautia*, host metabolism, and the onset of obesity. Following binning-based reconstruction of metagenome-assembled genomes (MAGs), we systematically investigated the horizontal dissemination of ARGs across microbiota taxa within the gut ecosystem. Interestingly, under prolonged intervention with tylosin, *Blautia* eventually harbored the largest number of antibiotic resistance gene contigs. This observation is consistent with the high carriage rate of vancomycin resistance genes in species within this genus; such genes are known to enhance the ability of bacteria to adapt to different environmental niches and colonization in the intestines of animals (Liu et al. 2021a; Liu et al. 2021b). A previous *meta*-analysis showed that feeding of tylosin increased in the proportion of macrolide-resistant *enterococci* in the bovine GI tract (Cazer et al. 2020). Another study proposed that *B. producta* colonized the gut with the assistance of *C. bolteae*, thereby facilitating the clearance of vancomycin-resistant *Enterococcus* (VRE) in the GI tract of patients (Caballero et al. 2017). Therefore, we hypothesize that *Blautia* acquired ARGs through horizontal gene transfer from other bacteria under the selection pressure of tylosin, and that *Blautia* strains may also transmit ARGs to other intestinal bacteria, posing environmental and human health threat (McInnes et al. 2020). These findings confirm that prolonged intervention with tylosin causes disturbances in the gut

microbiota, especially by altering microbiota structure as well as gut metabolite composition, potentially triggering onset of physiological and metabolic disorders such as obesity; these events also lead to concentration of resistance genes in specific bacterial strains due to reduced microbial diversity, promoting development of AMR.

In addition to the direct impact on gut microbiota, transcriptome analysis also revealed alterations in gene expression within the ileum tissue of the GI tract. The small intestine, which is primarily responsible for nutrient absorption, may exhibit enhanced nutrient uptake and utilization upon exposure to AGPs which may cause a reduction in intestinal mucosal thickness (Judkins et al. 2020; Rahman et al. 2022). KEGG pathway annotation revealed upregulation in energy metabolism and disease development pathways, including those associated with non-alcoholic fatty liver disease and diabetic cardiomyopathy; these data are consistent with the pathological changes observed in the animal experiments. At the genetic level (Fig. S5a), expression of Hub genes linked to mitochondrial activity, such as *mt-Co1*, *mt-Co2*, and *mt-Co3* (encoding mitochondrial cytochrome *c* oxidase), *mt-Atp6* (mitochondrial ATP synthase), and *mt-Nd1* and *mt-Nd2* (mitochondrial NADH dehydrogenase), were found to be upregulated, suggesting an imbalance in energy metabolism upon tylosin treatment (Cerqua et al. 2021; Lim et al. 2016). A nested case-control study previously showed that methylation of mitochondrial DNA genes like *mt-Co1* and *mt-Co3* could serve as biomarkers for cardiovascular disease in overweight and obese patients (Corsi et al. 2020). Intriguingly, downregulation in the expression of genes and pathways related to inflammation and immunity was observed in the tylosin treatment. Intestinal epithelial cells are known to secrete various immune factors to maintain gut health (Kayama et al. 2020). Previous studies have shown that AGPs can downregulate the expression of intestinal inflammatory factors, such as *IL-1β* and *IL-17A*, during microbial infections, thereby reducing severe inflammatory responses and aiding in the maintenance of host health (Brüssow 2015; Oh et al. 2019). However, it is not clear whether AGPs continue to suppress these inflammatory factors and immune functions in the absence of pathogens. Niewold *et al.,* suggested that AGPs might inhibit the production of metabolic mediators by inflammatory cells, promoting growth independent of gut microbes (Niewold 2007). Furthermore, prolonged antibiotic treatment was found to disrupt innate immunity and gut homeostasis, potentially leading to inflammatory bowel diseases (Wlodarska and Finlay 2010). Therefore, tylosin-induced immunosuppression may not always be beneficial and could increase mortality risk during infections by highly pathogenic microorganisms (Wallis et al. 2023). All in all, our data confirms that tylosin disrupts energy metabolism in the GI tract, causing obesity and liver diseases upon prolonged treatment. Furthermore, the ability of tylosin to suppress the expression of inflammatory factors may be either beneficial or detrimental, depending on whether the host is being infected by microbial pathogens during the treatment process. As our data showed that tylosin may cause reduction in host immunity, we believe that any benefits of the drug brought about by suppression of life-threatening inflammation induced by microbial infections are counteracted by the lowered immune responses in the host upon prolonged exposure to this drug. The gut-liver axis plays a critical role in maintaining systemic physiological, immune, and metabolic balance (Tilg et al. 2022). Changes in the level of intestinal metabolites, such as bile acids and SCFAs, can disrupt the ability of the liver to regulate lipid metabolism (Hu et al. 2021; Luo et al. 2023). Moreover, as a key organ that plays a role in drug metabolism, excessive drug intake challenges the detoxification capacity of the liver, impairing liver functions and indirectly affecting other crucial metabolic pathways (Lai et al. 2022; Tilg et al. 2021). In this study, gene and metabolic profiles of the liver were found to be altered significantly upon tylosin intervention. Initially, from the DEGs annotated by KEGG, we observed upregulation of the arachidonic acid (AA) metabolism pathway. In a previous study, the administration of florfenicol, a broad-spectrum antibiotic, also can diminish SCFAs production by disrupting gut microbiota (Zhao et al. 2024). These changes impaired hepatic fatty acid synthesis, degradation, and transformation- including AA metabolism-while dysregulated SCFAs signaling pathways promoted insulin resistance, thereby exacerbating hepatic lipid accumulation and AA dyshomeostasis. AA is also closely linked to various physiological metabolic activities, including activation of the cyclooxygenase (COX) pathway which is responsible for triggering the onset of inflammation and NAFLD (Sztolsztener et al. 2020), as well as induction of the lipoxygenase (LOX) pathway, whose products, leukotrienes (such as LTA4), are related to hepatic inflammatory responses (Shimizu et al. 1984). Besides, current evidence suggests that leukotriene (LTB4), downstream metabolites of LTA4, serve as a critical mediator in metabolic disorders such as obesity and diabetes, actively contributing to the pathogenesis of lipid metabolism dysregulation (Haeggström 2018; Ramalho et al. 2019). A recent study showed that LTB4 can increase intracellular cAMP levels, thereby activating the IRE1α-XBP1 endoplasmic reticulum pathway, which in turn leads to the accumulation of lipids in the liver and onset of NAFLD (Liu et al. 2023b). On the other hand, we noted the pathway "Drug metabolism – other enzymes," which is related to the potential of tylosin to disrupt host metabolism, was down-regulated. Fortunately, the CytoHubba software helped us identify *Cyp2c47*, *Cyp2c50*, and *Cyp2c54*, which are members of the cytochrome P450 (CYP) superfamily, from the upregulated Hub genes (Fig. S6a). Enzymes of the CYP family primarily participate in drug metabolism in the liver, facilitating the conversion of drugs into more easily excretable active substances (Song et al. 2021). In addition, Cyp2c family enzymes convert AA into epoxyeicosatrienoic acids (EETs) via the epoxidation pathway, contributing to inflammatory responses (Spector et al. 2004). Based on this observation, we hypothesize that tylosin initially upregulates CYP family gene expression in the liver to coordinate drug metabolism, but it also positively activates the COX and LOX pathways, thereby stimulating the production of AA. However, as the intervention progresses, liver cells are damaged, diminishing their capacity for drug metabolism, but accumulation of other metabolic products such as leukotrienes disrupts lipid metabolism in the liver and eventually causes metabolic disorders (Fig. 6**d**).

Results of integrative transcriptomic and metabolomic analysis support our hypothesis, as the relative increase in the abundance of the key metabolite LTA4 confirms the activation of the LOX pathway. Additionally, we identified 20-CoA-20-oxo-LTB4 in the liver through analysis of the metabolomic data; this compound, which is produced from LTB4 via lipid ω-oxidation, may also intervene in organ lipid metabolism. Interestingly, an increase in the downstream leukotrienes, namely LTC4, LTD4, and LTE4, was also detectable in the plasma metabolomic profile (Table S8). This finding corroborates the imbalance in multiple AA-mediated metabolic pathways in the liver, allowing related metabolites to enter the bloodstream through the hepatic portal vein, posing a threat to the normal functioning of other organs. Furthermore, as inflammatory mediators, they echo the previously observed suppression of inflammation in the small intestine, possibly due to continuous immune system stimulation which cause functional imbalance and decline (Albillos et al. 2022; Yang et al. 2017). Thus, our results demonstrate that impairment of liver function and induction of disorder in multiple metabolic pathways during tylosin treatment was mediated by AA and LTA4, which act by severely disrupting lipid metabolism and suppressing host immune function. In a parallel AGP intervention study utilizing lincomycin, we observed analogous outcomes, further corroborating the central hypothesis of this investigation (Ni et al. 2024).

A previous study demonstrated that over 28% of tylosin intake in animals is excreted in their manures, with residual antibiotics directly contaminating the soil environment. These drug residues may promote the development of AMR in microorganisms and cross-species transmission of ARGs (Chen et al. 2018). Furthermore, animal wastes can be utilized as manure for crop production, allowing antibiotic residues to be accumulated and enriched in the human body (Pan and Chu 2017). Both meat products from animals fed with AGPs and crops contaminated

with such compounds could potentially pose health risks to humans, potentially causing a range of metabolic diseases as revealed in this study.

5. Conclusions

The physiological response of an animal host to tylosin upon exposure to this agent for a prolonged period was found. Integrative multi-omics analyses show that tylosin disrupts the structure of the gut microbiome and promotes the development of AMR; we also revealed metabolic dysregulation in the liver due to activation of the arachidonic acid metabolism pathway upon tylosin treatment. The drug was also found to cause immune suppression, and early onset of T2DM and NAFLD metabolic disorders. These findings suggest that the weight gain induced by the use of AGPs bears the cost of compromising animal health and welfare. These health risks may be transmitted to humans via food intake and environmental exposure. The potential adverse consequences of using AGPs in livestock production should be addressed and a search for alternative AGPs is urgently needed.

CRediT authorship contribution statement

Hongyuhang Ni: Writing – review & editing, Writing – original draft, Visualization, Methodology, Investigation, Formal analysis, Data curation, Conceptualization. **Jing Wang:** Writing – original draft, Methodology, Investigation, Formal analysis, Data curation. **Haoze Wu:** Writing – original draft, Methodology, Investigation, Formal analysis, Data curation. **Bill Kwan-wai Chan:** Investigation, Data curation. **Kaichao Chen:** Investigation. **Han Wang:** Investigation. **Edward Wai-Chi Chan:** Writing – review & editing, Writing – original draft, Conceptualization. **Fuyong Li:** Writing – review & editing, Conceptualization. **Sheng Chen:** Writing – review & editing, Writing – original draft, Supervision, Funding acquisition, Conceptualization.

Declaration of competing interest

The authors declare that they have no known competing financial interests or personal relationships that could have appeared to influence the work reported in this paper.

Acknowledgments

This study was funded by the Theme-Based Research Scheme (T11-104/22-R) and the Research Impact Fund (R1011-23) from the Research Grant Council of the Hong Kong Government. Parts of Fig. 6 were drawn using pictures from Servier Medical Art (https://smart.servier.com/), which are licensed under a Creative Commons Attribution 4.0 License. Authors also acknowledged BioRender (https://www.biorender.com/) for creation of graphical abstract.

Appendix A. Supplementary material

Supplementary data to this article can be found online at https://doi.org/10.1016/j.envint.2025.109684.

Data availability

The raw 16S rRNA gene sequence data of gut microbiota collected from the test mice are available in the Genbank under accession number PRJNA1164402. The metagenomic sequencing data of fecal samples from mice are accessible under accession number PRJNA1164486. The transcriptomic sequencing datasets for mouse ileum and liver tissues are available under accession number PRJNA1164642. Lastly, the metabolomic sequencing datasets for the liver and plasma samples of mice treated with tylosin are listed under OMIX ID OMIX007475, which is associated with BioProject PRJCA030446.

References

Albillos, A., Martin-Mateos, R., Van der Merwe, S., Wiest, R., Jalan, R., Álvarez-Mon, M., 2022. Cirrhosis-associated immune dysfunction. Nat. Rev. Gastroenterol. Hepatol. 19, 112–134. https://doi.org/10.1038/s41575-021-00520-7.

Alcock, B.P., Huynh, W., Chalil, R., Smith, K.W., Raphenya, A.R., Wlodarski, M.A., Edalatmand, A., Petkau, A., Syed, S.A., Tsang, K.K., 2023. CARD 2023: expanded curation, support for machine learning, and resistome prediction at the comprehensive antibiotic resistance database. Nucleic Acids Res. 51, D690–D699. https://doi.org/10.1093/nar/gkac920.

Alqahtani, F., Albekairi, T.H., Aleidi, S.M., AlMalki, R.H., Ali, Y.S.M., Almutairi, M.M., Alshammari, M.A., Alshememry, A.K., Rahman, A.M.A., 2024. Metabolomics and pathways analyses in traumatic brain injury animal model. J. King Saud Univ.-Sci. 36, 103470. https://doi.org/10.1016/j.jksus.2024.103470.

Ardui, S., Ameur, A., Vermeesch, J.R., Hestand, M.S., 2018. Single molecule real-time (SMRT) sequencing comes of age: applications and utilities for medical diagnostics. Nucleic Acids Res. 46, 2159–2168. https://doi.org/10.1093/nar/gky066.

Ayalew, H., Zhang, H., Wang, J., Wu, S., Qiu, K., Qi, G., Tekeste, A., Wassie, T., Chanie, D., 2022. Potential feed additives as antibiotic alternatives in broiler production. Front. Vet. Sci. 9, 916473. https://doi.org/10.3389/fvets.2022.916473.

Bachmanov, A.A., Reed, D.R., Beauchamp, G.K., Tordoff, M.G., 2002. Food Intake, Water Intake, and Drinking Spout Side Preference of 28 Mouse Strains. Behav. Genet. 32, 435–443. https://doi.org/10.1023/A:1020884312053.

Biely, J., March, B., 1951. The effect of aureomycin and vitamins on the growth rate of chicks. Science 114, 330–331. https://doi.org/10.1126/science.114.2961.330.b.

Bolger, A.M., Lohse, M., Usadel, B., 2014. Trimmomatic: a flexible trimmer for Illumina sequence data. Bioinformatics 30, 2114–2120. https://doi.org/10.1093/bioinformatics/btu170.

Brown, K., Zaytsoff, S.J.M., Uwiera, R.R.E., Inglis, G.D., 2016. Antimicrobial growth promoters modulate host responses in mice with a defined intestinal microbiota. Sci. Rep. 6, 38377. https://doi.org/10.1038/srep38377.

Brüssow, H., 2015. Growth promotion and gut microbiota: insights from antibiotic use. Environ. Microbiol. 17, 2216–2227. https://doi.org/10.1111/1462-2920.12786.

Butaye, P., Devriese, L.A., Haesebrouck, F., 2003. Antimicrobial Growth Promoters used in Animal Feed: Effects of less well known Antibiotics on Gram-positive Bacteria. Clin. Microbiol. Rev. 16, 175–188. https://doi.org/10.1128/cmr.16.2.175-188.2003.

Caballero, S., Kim, S., Carter, R.A., Leiner, I.M., Sušac, B., Miller, L., Kim, G.J., Ling, L., Pamer, E.G., 2017. Cooperating commensals restore colonization resistance to vancomycin-resistant Enterococcus faecium. Cell Host Microbe 21, 592–602.e594. https://doi.org/10.1016/j.chom.2017.04.002.

Casimiro, I., Stull, N.D., Tersey, S.A., Mirmira, R.G., 2021. Phenotypic sexual dimorphism in response to dietary fat manipulation in C57BL/6J mice. J Diabetes Complicat. 35, 107795. https://doi.org/10.1016/j.jdiacomp.2020.107795.

Cazer, C.L., Eldermire, E.R.B., Lhermie, G., Murray, S.A., Scott, H.M., Gröhn, Y.T., 2020. The effect of tylosin on antimicrobial resistance in beef cattle enteric bacteria: a systematic review and meta-analysis. Prev. Vet. Med. 176, 104934. https://doi.org/10.1016/j.prevetmed.2020.104934.

Cerqua, C., Buson, L., Trevisson, E., 2021. Mutations in Assembly Factors Required for the Biogenesis of Mitochondrial respiratory Chain. In: Navas, P., Salviati, L. (Eds.), Mitochondrial Diseases: Theory, Diagnosis and Therapy. Springer International Publishing, Cham. https://doi.org/10.1007/978-3-030-70147-5_2.

Chanda, W., Jiang, H., Liu, S.-J., 2024. The ambiguous correlation of blautia with obesity: a systematic review. Microorganisms 12, 1768. https://doi.org/10.3390/microorganisms12091768.

Chen, C., Ray, P., Knowlton, K.F., Pruden, A., Xia, K., 2018. Effect of composting and soil type on dissipation of veterinary antibiotics in land-applied manures. Chemosphere 196, 270–279. https://doi.org/10.1016/j.chemosphere.2017.12.161.

Chen, J., Cheng, J., Chen, X., Inoue, M., Liu, Y., Song, C.-X., 2022a. Whole-genome long-read TAPS deciphers DNA methylation patterns at base resolution using PacBio SMRT sequencing technology. Nucleic Acids Res. 50, e104–e. https://doi.org/10.1093/nar/gkac612.

Chen, R.-A., Wu, W.-K., Panyod, S., Liu, P.-Y., Chuang, H.-L., Chen, Y.-H., Lyu, Q., Hsu, H.-C., Lin, T.-L., Shen, T.-C.-D., 2022b. Dietary exposure to antibiotic residues facilitates metabolic disorder by altering the gut microbiota and bile acid composition. Msystems 7, e00172–00122. https://doi.org/10.1128/msystems.00172-22.

Chen, S., 2023. Ultrafast one-pass FASTQ data preprocessing, quality control, and deduplication using fastp. iMeta 2, e107.

Cheng, Y.-C., Liu, J.-R., 2020. Effect of lactobacillus rhamnosus gg on energy metabolism, leptin resistance, and gut microbiota in mice with diet-induced obesity. Nutrients 12, 2557. https://doi.org/10.3390/nu12092557.

Chin, C.-H., Chen, S.-H., Wu, H.-H., Ho, C.-W., Ko, M.-T., Lin, C.-Y., 2014. cytoHubba: identifying hub objects and sub-networks from complex interactome. BMC Syst. Biol. 8, 1–7. https://doi.org/10.1186/1752-0509-8-S4-S11.

Cline, M.S., Smoot, M., Cerami, E., Kuchinsky, A., Landys, N., Workman, C., Christmas, R., Avila-Campilo, I., Creech, M., Gross, B., 2007. Integration of biological networks and gene expression data using Cytoscape. Nat. Protoc. 2, 2366–2382. https://doi.org/10.1038/nprot.2007.324.

Corsi, S., Iodice, S., Vigna, L., Cayir, A., Mathers, J.C., Bollati, V., Byun, H.-M., 2020. Platelet mitochondrial DNA methylation predicts future cardiovascular outcome in adults with overweight and obesity. Clin Epigenet. 12, 29. https://doi.org/10.1186/s13148-020-00825-5.

Cui, Z., Liu, T., Wen, Y., Li, W., Xu, J., Chen, Y., Chen, D., Zhu, Y., 2024. Oral administration of cranberry-derived exosomes attenuates murine premature ovarian failure in association with changes in the specific gut microbiota and diminution in

ovarian granulosa cell PANoptosis. Food Funct. 15, 11697–11714. https://doi.org/10.1039/D4FO03468F.
De Liguoro, M., Cibin, V., Capolongo, F., Halling-Sørensen, B., Montesissa, C., 2003. Use of oxytetracycline and tylosin in intensive calf farming: evaluation of transfer to manure and soil. Chemosphere 52, 203–212. https://doi.org/10.1016/S0045-6535(03)00284-4.
Dixon, P., 2003. VEGAN, a package of R functions for community ecology. J. Veg. Sci. 14, 927–930. https://doi.org/10.1111/j.1654-1103.2003.tb02228.x.
Dong, H., Chen, Y., Wang, J., Zhang, Y., Zhang, P., Li, X., Zou, J., Zhou, A., 2021. Interactions of microplastics and antibiotic resistance genes and their effects on the aquaculture environments. J. Hazard. Mater. 403, 123961. https://doi.org/10.1016/j.jhazmat.2020.123961.
Dueholm, M.S., Andersen, K.S., McIlroy, S.J., Kristensen, J.M., Yashiro, E., Karst, S.M., Albertsen, M., Nielsen, P.H., 2020. Generation of comprehensive ecosystem-specific reference databases with species-level resolution by high-throughput full-length 16S rRNA gene sequencing and automated taxonomy assignment (AutoTax). MBio 11. https://doi.org/10.1128/mbio.01557-20.
Evangelista, A.G., Corrêa, J.A.F., Pinto, A.C.S.M., Luciano, F.B., 2022. The impact of essential oils on antibiotic use in animal production regarding antimicrobial resistance–a review. Crit. Rev. Food Sci. Nutr. 62, 5267–5283. https://doi.org/10.1080/10408398.2021.1883548.
Feng, G., Huang, H., Chen, Y., 2021. Effects of emerging pollutants on the occurrence and transfer of antibiotic resistance genes: a review. J. Hazard. Mater. 420, 126602. https://doi.org/10.1016/j.jhazmat.2021.126602.
Feng, P., Yang, J., Zhao, S., Ling, Z., Han, R., Wu, Y., Salama, E.-S., Kakade, A., Khan, A., Jin, W., 2022. Human supplementation with Pediococcus acidilactici GR-1 decreases heavy metals levels through modifying the gut microbiota and metabolome. npj Biofilms Microbiomes 8, 63. https://doi.org/10.1038/s41522-022-00326-8.
Fernández Miyakawa, M.E., Casanova, N.A., Kogut, M.H., 2024. How did antibiotic growth promoters increase growth and feed efficiency in poultry? Poult. Sci. 103, 103278. https://doi.org/10.1016/j.psj.2023.103278.
Founou, L.L., Founou, R.C., Essack, S.Y., 2016. Antibiotic Resistance in the Food Chain: a developing Country-Perspective. Front. Microbiol. 7. https://doi.org/10.3389/fmicb.2016.01881.
Gao, H., Shu, Q., Chen, J., Fan, K., Xu, P., Zhou, Q., Li, C., Zheng, H., 2019. Antibiotic exposure has sex-dependent effects on the gut microbiota and metabolism of short-chain fatty acids and amino acids in mice. Msystems 4, 10–1128. https://doi.org/10.1128/msystems.00048-19.
Geng, J., Ni, Q., Sun, W., Li, L., Feng, X., 2022. The links between gut microbiota and obesity and obesity related diseases. Biomed. Pharmacother. 147, 112678. https://doi.org/10.1016/j.biopha.2022.112678.
Geng, P., Zhao, N., Zhou, Y., Harris, R.S., Ge, Y., 2025. Faecalibacterium prausnitzii regulates carbohydrate metabolic functions of the gut microbiome in C57BL/6 mice. Gut Microbes 17, 2455503. https://doi.org/10.1080/19490976.2025.2455503.
Gonzalez Ronquillo, M., Angeles Hernandez, J.C., 2017. Antibiotic and synthetic growth promoters in animal diets: Review of impact and analytical methods. Food Control 72, 255–267. https://doi.org/10.1016/j.foodcont.2016.03.001.
Gurevich, A., Saveliev, V., Vyahhi, N., Tesler, G., 2013. QUAST: quality assessment tool for genome assemblies. Bioinformatics 29, 1072–1075. https://doi.org/10.1093/bioinformatics/btt086.
Haeggström, J.Z., 2018. Leukotriene biosynthetic enzymes as therapeutic targets. J. Clin. Invest. 128, 2680–2690. https://doi.org/10.1172/JCI97945.
Hall, M., Beiko, R.G., 2018. 16S rRNA gene analysis with QIIME2. Microbiome analysis: methods and protocols. 113–129. doi: 10.1007/978-1-4939-8728-3_8.
Hallenberg, G.S., Jiwakanon, J., Angkititrakul, S., Kang-Air, S., Osbjer, K., Lunha, K., Sunde, M., Järhult, J.D., Van Boeckel, T.P., Rich, K.M., 2020. Antibiotic use in pig farms at different levels of intensification—farmers' practices in northeastern Thailand. PLoS One 15, e0243099. https://doi.org/10.1371/journal.pone.0243099.
Heo, J., Seo, M., Park, H., Lee, W.K., Guan, L.L., Yoon, J., Caetano-Anolles, K., Ahn, H., Kim, S.-Y., Kang, Y.-M., Cho, S., Kim, H., 2016. Gut microbiota modulated by probiotics and garcinia cambogia extract correlate with weight gain and adipocyte sizes in high fat-fed mice. Sci. Rep. 6, 33566. https://doi.org/10.1038/srep33566.
Hioki, C., Yoshida, T., Kogure, A., Yoshimoto, K., Shimatsu, A., 2010. Growth hormone administration controls body composition associated with changes of thermogenesis in obese KK-Ay mice. Open Endocrinol. J. 4. https://doi.org/10.2174/1874216501004010003.
Hu, Y., Li, C., Hou, Y., 2021. Possible regulation of liver glycogen structure through the gut-liver axis by resistant starch: a review. Food Funct. 12, 11154–11164. https://doi.org/10.1039/D1FO02416G.
Huang, B.-M., Zha, Q.-L., Chen, T.-B., Xiao, S.-Y., Xie, Y., Luo, P., Wang, Y.-P., Liu, L., Zhou, H., 2018. Discovery of markers for discriminating the age of cultivated ginseng by using UHPLC-QTOF/MS coupled with OPLS-DA. Phytomedicine 45, 8–17. https://doi.org/10.1016/j.phymed.2018.03.011.
Ishikawa, N.K., Touno, E., Higashiyama, Y., Sasamoto, M., Soma, M., Yoshida, N., Ito, A., Umita, T., 2018. Determination of tylosin excretion from sheep to assess tylosin spread to agricultural fields by manure application. Sci. Total Environ. 633, 399–404. https://doi.org/10.1016/j.scitotenv.2018.03.216.
Judkins, T.C., Archer, D.L., Kramer, D.C., Solch, R.J., 2020. Probiotics, nutrition, and the small intestine. Curr. Gastroenterol. Rep. 22, 1–8. https://doi.org/10.1007/s11894-019-0740-3.
Kanehisa, M., Goto, S., 2000. KEGG: kyoto encyclopedia of genes and genomes. Nucleic Acids Res. 28, 27–30. https://doi.org/10.1093/nar/28.1.27.
Kang, D.D., Froula, J., Egan, R., Wang, Z., 2015. MetaBAT, an efficient tool for accurately reconstructing single genomes from complex microbial communities. PeerJ 3, e1165.
Kappel, B.A., De Angelis, L., Heiser, M., Ballanti, M., Stoehr, R., Goettsch, C., Mavilio, M., Artati, A., Paoluzi, O.A., Adamski, J., Mingrone, G., Staels, B., Burcelin, R., Monteleone, G., Menghini, R., Marx, N., Federici, M., 2020. Cross-omics analysis revealed gut microbiome-related metabolic pathways underlying atherosclerosis development after antibiotics treatment. Mol. Metab. 36, 100976. https://doi.org/10.1016/j.molmet.2020.100976.
Kaufman, A., Abuqayyas, L., Denney, W.S., Tillman, E.J., Rolph, T., 2020. AKR-001, an Fc-FGF21 analog, showed sustained pharmacodynamic effects on insulin sensitivity and lipid metabolism in type 2 diabetes patients. Cell Rep. Med. 1. https://doi.org/10.1016/j.xcrm.2020.100057.
Kayama, H., Okumura, R., Takeda, K., 2020. Interaction between the microbiota, epithelia, and immune cells in the intestine. Annu. Rev. Immunol. 38, 23–48. https://doi.org/10.1146/annurev-immunol-070119-115104.
Kiani, A.K., Pheby, D., Henehan, G., Brown, R., Sieving, P., Sykora, P., Marks, R., Falsini, B., Capodicasa, N., Miertus, S., 2022. Ethical considerations regarding animal experimentation. J. Prev. Med. Hyg. 63, E255. https://doi.org/10.15167/2421-4248/jpmh2022.63.2S3.2768.
Kim, D., Paggi, J.M., Park, C., Bennett, C., Salzberg, S.L., 2019. Graph-based genome alignment and genotyping with HISAT2 and HISAT-genotype. Nat. Biotechnol. 37, 907–915. https://doi.org/10.1038/s41587-019-0201-4.
Klancic, T., Laforest-Lapointe, I., Choo, A., Nettleton, J.E., Chleilat, F., Noye Tuplin, E. W., Alukic, E., Cho, N.A., Nicolucci, A.C., Arrieta, M.-C., Reimer, R.A., 2020. Prebiotic oligofructose prevents antibiotic-induced obesity risk and improves metabolic and gut microbiota profiles in rat dams and offspring. Mol. Nutr. Food Res. 64, 2000288. https://doi.org/10.1002/mnfr.202000288.
Kline, A., Pinckney, J.L., 2016. Size-selective toxicity effects of the antimicrobial tylosin on estuarine phytoplankton communities. Environ. Pollut. 216, 806–810. https://doi.org/10.1016/j.envpol.2016.06.050.
Lai, Y., Chu, X., Di, L., Gao, W., Guo, Y., Liu, X., Lu, C., Mao, J., Shen, H., Tang, H., 2022. Recent advances in the translation of drug metabolism and pharmacokinetics science for drug discovery and development. Acta Pharm. Sin. B 12, 2751–2777. https://doi.org/10.1016/j.apsb.2022.03.009.
Langmead, B., Salzberg, S.L., 2012. Fast gapped-read alignment with Bowtie 2. Nat Meth. 9, 357–359. https://doi.org/10.1038/nmeth.1923.
Lee, E.-B., Lee, G.-Y., Hossain, M.A., Awji, E.G., Park, S.-C., 2024. Gut microbiome perturbation and its correlation with tylosin pharmacokinetics in healthy and infected pigs. Sci. Rep. 14, 18670. https://doi.org/10.1038/s41598-024-69566-2.
Li, D., Luo, R., Liu, C.-M., Leung, C.-M., Ting, H.-F., Sadakane, K., Yamashita, H., Lam, T.-W., 2016. MEGAHIT v1. 0: a fast and scalable metagenome assembler driven by advanced methodologies and community practices. Methods 102, 3–11. https://doi.org/10.1016/j.ymeth.2016.02.020.
Li, H.-Y., Huang, S.-Y., Zhou, D.-D., Xiong, R.-G., Luo, M., Saimaiti, A., Han, M.-K., Gan, R.-Y., Zhu, H.-L., Li, H.-B., 2023. Theabrownin inhibits obesity and non-alcoholic fatty liver disease in mice via serotonin-related signaling pathways and gut-liver axis. J. Adv. Res. 52, 59–72. https://doi.org/10.1016/j.jare.2023.01.008.
Li, Q., Lu, D., Sun, H., Guo, J., Mo, J., 2021. Tylosin toxicity in the alga Raphidocelis subcapitata revealed by integrated analyses of transcriptome and metabolome: Photosynthesis and DNA replication-coupled repair. Aquat. Toxicol. 239, 105964. https://doi.org/10.1016/j.aquatox.2021.105964.
Li, W., Zhang, G., 2022. Detection and various environmental factors of antibiotic resistance gene horizontal transfer. Environ. Res. 212, 113267. https://doi.org/10.1016/j.envres.2022.113267.
Lim, S.C., Hroudová, J., Van Bergen, N.J., Sanchez, M.I.G.L., Trounce, I.A., McKenzie, M., 2016. Loss of mitochondrial DNA-encoded protein ND1 results in disruption of complex I biogenesis during early stages of assembly. FASEB J. 30, 2236–2248. https://doi.org/10.1096/fj.201500137R.
Litichevskiy, L., Considine, M., Gill, J., Shandar, V., Cox, T.O., Descamps, H.C., Wright, K.M., Amses, K.R., Dohnalová, L., Liou, M.J., Tetlak, M., Galindo-Fiallos, M. R., Wong, A.C., Lundgren, P., Kim, J., Uhr, G.T., Rahman, R.J., Mason, S., Merenstein, C., Bushman, F.D., Raj, A., Harding, F., Chen, Z., Prateek, G.V., Mullis, M., Deighan, A.G., Robinson, L., Tanes, C., Bittinger, K., Chakraborty, M., Bhatt, A.S., Li, H., Barnett, I., Davenport, E.R., Broman, K.W., Levy, M., Cohen, R.L., Botstein, D., Freund, A., Di Francesco, A., Churchill, G.A., Li, M., Thaiss, C.A., 2025. Gut metagenomes reveal interactions between dietary restriction, ageing and the microbiome in genetically diverse mice. Nat. Microbiol. 10, 1240–1257. https://doi.org/10.1038/s41564-025-01963-3.
Liu, B., Sträuber, H., Centler, F., Harms, H., da Rocha, U.N., Kleinsteuber, S., 2023a. Functional redundancy secures resilience of chain elongation communities upon pH shifts in closed bioreactor ecosystems. Environ. Sci. Technol. 57, 18350–18361. https://doi.org/10.1021/acs.est.2c09573.
Liu, M., Douthwaite, S., 2002. Resistance to the macrolide antibiotic tylosin is conferred by single methylations at 23S rRNA nucleotides G748 and A2058 acting in synergy. Proc. Natl. Acad. Sci. 99, 14658–14663. https://doi.org/10.1073/pnas.232580599.
Liu, X., Guo, W., Cui, S., Tang, X., Zhao, J., Zhang, H., Mao, B., Chen, W., 2021a. A comprehensive assessment of the safety of blautia producta DSM 2950. Microorganisms 9, 908. https://doi.org/10.3390/microorganisms9050908.
Liu, X., Mao, B., Gu, J., Wu, J., Cui, S., Wang, G., Zhao, J., Zhang, H., Chen, W., 2021b. Blautia—a new functional genus with potential probiotic properties? Gut Microbes 13, 1875796. https://doi.org/10.1080/19490976.2021.1875796.
Liu, X., Wang, K., Wang, L., Kong, L., Hou, S., Wan, Y., Ma, C., Chen, J., Xing, X., Xing, C., 2023b. Hepatocyte leukotriene B4 receptor 1 promotes NAFLD development in obesity. Hepatology 78, 562–577. https://doi.org/10.1002/hep.32708.
Love, M.I., Huber, W., Anders, S., 2014. Moderated estimation of fold change and dispersion for RNA-seq data with DESeq2. Genome Biol. 15, 1–21. https://doi.org/10.1186/s13059-014-0550-8.

Luan, Y., Zhao, J., Han, H., Shen, J., Tang, S., Cheng, L., 2021. Toxicologic effect and transcriptome analysis for short-term orally dosed enrofloxacin combined with two veterinary antimicrobials on rat liver. Ecotoxicol. Environ. Saf. 220, 112398. https://doi.org/10.1016/j.ecoenv.2021.112398.

Luo, L., Chang, Y., Sheng, L., 2023. Gut-liver axis in the progression of nonalcoholic fatty liver disease: from the microbial derivatives-centered perspective. Life Sci. 321, 121614. https://doi.org/10.1016/j.lfs.2023.121614.

Mahana, D., Trent, C.M., Kurtz, Z.D., Bokulich, N.A., Battaglia, T., Chung, J., Müller, C. L., Li, H., Bonneau, R.A., Blaser, M.J., 2016. Antibiotic perturbation of the murine gut microbiome enhances the adiposity, insulin resistance, and liver disease associated with high-fat diet. Genome Med. 8, 48. https://doi.org/10.1186/s13073-016-0297-9.

Maron, D.F., Smith, T.J.S., Nachman, K.E., 2013. Restrictions on antimicrobial use in food animal production: an international regulatory and economic survey. Glob. Health 9, 48. https://doi.org/10.1186/1744-8603-9-48.

Martin, M., 2011. Cutadapt removes adapter sequences from high-throughput sequencing reads. Embnet Journal. 17. https://doi.org/10.14806/ej.17.1.200.

McInnes, R.S., McCallum, G.E., Lamberte, L.E., van Schaik, W., 2020. Horizontal transfer of antibiotic resistance genes in the human gut microbiome. Curr. Opin. Microbiol. 53, 35–43. https://doi.org/10.1016/j.mib.2020.02.002.

Ni, H., Wu, H., Wang, J., Chan, B.K.-W., Chen, K., Chan, E.W.-C., Li, F., Chen, S., 2024. Lincomycin as a growth-promoting antibiotic induces metabolic and immune dysregulation in animals. Sci. Total Environ. 957, 177780. https://doi.org/10.1016/j.scitotenv.2024.177780.

Niewold, T., 2007. The nonantibiotic anti-inflammatory effect of antimicrobial growth promoters, the real mode of action? A Hypothesis. Poult Sci. 86, 605–609. https://doi.org/10.1093/ps/86.4.605.

Oh, S., Lillehoj, H.S., Lee, Y., Bravo, D., Lillehoj, E.P., 2019. Dietary antibiotic growth promoters down-regulate intestinal inflammatory cytokine expression in chickens challenged with LPS or Co-infected with eimeria maxima and clostridium perfringens. Front. Vet. Sci. 6. https://doi.org/10.3389/fvets.2019.00420.

Pan, M., Chu, L.M., 2017. Fate of antibiotics in soil and their uptake by edible crops. Sci. Total Environ. 599–600, 500–512. https://doi.org/10.1016/j.scitotenv.2017.04.214.

Patyra, E., Kwiatek, K., Nebot, C., Gavilán, R.E., 2020. Quantification of veterinary antibiotics in pig and poultry feces and liquid manure as a non-invasive method to monitor antibiotic usage in livestock by liquid chromatography mass-spectrometry. Molecules 25, 3265. https://doi.org/10.3390/molecules25143265.

Peiseler, M., Schwabe, R., Hampe, J., Kubes, P., Heikenwälder, M., Tacke, F., 2022. Immune mechanisms linking metabolic injury to inflammation and fibrosis in fatty liver disease – novel insights into cellular communication circuits. J. Hepatol. 77, 1136–1160. https://doi.org/10.1016/j.jhep.2022.06.012.

Pokharel, S., Shrestha, P., Adhikari, B., 2020. Antimicrobial use in food animals and human health: time to implement 'one health'approach. Antimicrob. Resist. Infect. Control 9, 1–5. https://doi.org/10.1186/s13756-020-00847-x.

Powell, J.E., Carver, Z., Leonard, S.P., Moran, N.A., 2021. Field-realistic tylosin exposure impacts honey bee microbiota and pathogen Susceptibility, which is ameliorated by native gut probiotics. Microbiol. Spectrum 9. https://doi.org/10.1128/spectrum.00103-00121.

Quarato, E.R., Salama, N.A., Li, A.J., Smith, C.O., Zhang, J., Kawano, Y., McArthur, M., Liesveld, J.L., Becker, M.W., Elliott, M.R., Eliseev, R.A., Calvi, L.M., 2023. Efferocytosis by bone marrow mesenchymal stromal cells disrupts osteoblastic differentiation via mitochondrial remodeling. Cell Death Dis. 14, 428. https://doi.org/10.1038/s41419-023-05931-9.

Rachdaoui, N., 2020. Insulin: the friend and the foe in the development of type 2 diabetes mellitus. Int. J. Mol. Sci. 21, 1770. https://doi.org/10.3390/ijms21051770.

Rahman, M.R.T., Fliss, I., Biron, E., 2022. Insights in the development and uses of alternatives to antibiotic growth promoters in poultry and swine production. Antibiotics 11, 766. https://doi.org/10.3390/antibiotics11060766.

Ramalho, T., Ramalingam, L., Filgueiras, L., Festuccia, W., Jancar, S., Moustaid-Moussa, N., 2019. Leukotriene-B4 modulates macrophage metabolism and fat loss in type 1 diabetic mice. J. Leukoc. Biol. 106, 665–675. https://doi.org/10.1002/JLB.MA1218-477RR.

Ramirez, J., Guarner, F., Bustos Fernandez, L., Maruy, A., Sdepanian, V.L., Cohen, H., 2020. Antibiotics as major disruptors of gut microbiota. Front. Cell. Infect. Microbiol. 10, 572912. https://doi.org/10.3389/fcimb.2020.572912.

Rushing, B.R., McRitchie, S., Arbeeva, L., Nelson, A.E., Azcarate-Peril, M.A., Li, Y.Y., Qian, Y., Pathmasiri, W., Sumner, S.C.J., Loeser, R.F., 2022. Fecal metabolomics reveals products of dysregulated proteolysis and altered microbial metabolism in obesity-related osteoarthritis. Osteoarthritis Cartilage 30, 81–91. https://doi.org/10.1016/j.joca.2021.10.006.

Sarmah, A.K., Meyer, M.T., Boxall, A.B.A., 2006. A global perspective on the use, sales, exposure pathways, occurrence, fate and effects of veterinary antibiotics (VAs) in the environment. Chemosphere 65, 725–759. https://doi.org/10.1016/j.chemosphere.2006.03.026.

Shimizu, T., Rådmark, O., Samuelsson, B., 1984. Enzyme with dual lipoxygenase activities catalyzes leukotriene A4 synthesis from arachidonic acid. Proc. Natl. Acad. Sci. 81, 689–693. https://doi.org/10.1073/pnas.81.3.689.

Smith, C.A., Want, E.J., O'Maille, G., Abagyan, R., Siuzdak, G., 2006. XCMS: processing mass spectrometry data for metabolite profiling using nonlinear peak alignment, matching, and identification. Anal. Chem. 78, 779–787. https://doi.org/10.1021/ac051437y.

Song, Y., Li, C., Liu, G., Liu, R., Chen, Y., Li, W., Cao, Z., Zhao, B., Lu, C., Liu, Y., 2021. Drug-metabolizing cytochrome P450 enzymes have multifarious influences on treatment outcomes. Clin. Pharmacokinet. 60, 585–601. https://doi.org/10.1007/s40262-021-01001-5.

Spector, A.A., Fang, X., Snyder, G.D., Weintraub, N.L., 2004. Epoxyeicosatrienoic acids (EETs): metabolism and biochemical function. Prog. Lipid Res. 43, 55–90. https://doi.org/10.1016/S0163-7827(03)00049-3.

Steinegger, M., Söding, J., 2017. MMseqs2 enables sensitive protein sequence searching for the analysis of massive data sets. Nat. Biotechnol. 35, 1026–1028. https://doi.org/10.1038/nbt.3988.

Stojanov, S., Berlec, A., Štrukelj, B., 2020. The influence of probiotics on the firmicutes/bacteroidetes ratio in the treatment of obesity and inflammatory bowel disease. Microorganisms 8, 1715. https://doi.org/10.3390/microorganisms8111715.

Sun, Y., Guo, Y., Shi, M., Qiu, T., Gao, M., Tian, S., Wang, X., 2021. Effect of antibiotic type and vegetable species on antibiotic accumulation in soil-vegetable system, soil microbiota, and resistance genes. Chemosphere 263, 128099. https://doi.org/10.1016/j.chemosphere.2020.128099.

Szklarczyk, D., Franceschini, A., Kuhn, M., Simonovic, M., Roth, A., Minguez, P., Doerks, T., Stark, M., Muller, J., Bork, P., 2010. The STRING database in 2011: functional interaction networks of proteins, globally integrated and scored. Nucleic Acids Res. 39, D561–D568. https://doi.org/10.1093/nar/gkq973.

Sztolsztener, K., Chabowski, A., Harasim-Symbor, E., Bielawiec, P., Konstantynowicz-Nowicka, K., 2020. Arachidonic acid as an early indicator of inflammation during non-alcoholic fatty liver disease development. Biomolecules 10, 1133. https://doi.org/10.3390/biom10081133.

Tian, Y., Gui, W., Koo, I., Smith, P.B., Allman, E.L., Nichols, R.G., Rimal, B., Cai, J., Liu, Q., Patterson, A.D., 2020. The microbiome modulating activity of bile acids. Gut Microbes 11, 979–996. https://doi.org/10.1080/19490976.2020.1732268.

Tilg, H., Adolph, T.E., Dudek, M., Knolle, P., 2021. Non-alcoholic fatty liver disease: the interplay between metabolism, microbes and immunity. Nat. Metab. 3, 1596–1607. https://doi.org/10.1038/s42255-021-00501-9.

Tilg, H., Adolph, T.E., Trauner, M., 2022. Gut-liver axis: Pathophysiological concepts and clinical implications. Cell Metab. 34, 1700–1718. https://doi.org/10.1016/j.cmet.2022.09.017.

Uritskiy, G.V., DiRuggiero, J., Taylor, J., 2018. MetaWRAP—a flexible pipeline for genome-resolved metagenomic data analysis. Microbiome 6, 158. https://doi.org/10.1186/s40168-018-0541-1.

Vallianou, N., Dalamaga, M., Stratigou, T., Karampela, I., Tsigalou, C., 2021. Do antibiotics cause obesity through long-term alterations in the gut microbiome? a review of current evidence. Curr. Obes. Rep. 10, 244–262. https://doi.org/10.1007/s13679-021-00438-w.

Villanueva, R.A.M., Chen, Z.J., 2019. ggplot2: elegant graphics for data analysis. Taylor & Francis. https://doi.org/10.1080/15366367.2019.1565254.

Wallis, R.S., O'Garra, A., Sher, A., Wack, A., 2023. Host-directed immunotherapy of viral and bacterial infections: past, present and future. Nat. Rev. Immunol. 23, 121–133. https://doi.org/10.1038/s41577-022-00734-z.

Wang, G., Li, G., Chang, J., Kong, Y., Jiang, T., Wang, J., Yuan, J., 2021. Enrichment of antibiotic resistance genes after sheep manure aerobic heap composting. Bioresour. Technol. 323, 124620. https://doi.org/10.1016/j.biortech.2020.124620.

Wang, Y., Guo, A.-L., Xu, Y., Xu, X., Yang, L., Yang, Y., Chao, L., 2024. EHDPP induces proliferation inhibition and apoptosis to spermatocyte: Insights from transcriptomic and metabolomic profiles. Ecotoxicol. Environ. Saf. 284, 116878. https://doi.org/10.1016/j.ecoenv.2024.116878.

Wang, Y., Zhang, S., Hong, Q., Song, H., Yang, L., Yang, K., Xu, H., Yu, F., 2022. Characteristics, non-carcinogenic risk assessment and prediction by HYSPLIT of bioaerosol released from hospital and municipal sewage China. Ecotoxicol. Environ. Saf. 246, 114131. https://doi.org/10.1016/j.ecoenv.2022.114131.

Wen, R., Li, C., Zhao, M., Wang, H., Tang, Y., 2022. Withdrawal of antibiotic growth promoters in China and its impact on the foodborne pathogen Campylobacter coli of swine origin. Front. Microbiol. 13, 1004725. https://doi.org/10.3389/fmicb.2022.1004725.

Wlodarska, M., Finlay, B.B., 2010. Host immune response to antibiotic perturbation of the microbiota. Mucosal. Immunol. 3, 100–103. https://doi.org/10.1038/mi.2009.135.

Wu, Y.-W., Simmons, B.A., Singer, S.W., 2015. MaxBin 2.0: an automated binning algorithm to recover genomes from multiple metagenomic datasets. Bioinformatics 32, 605–607. https://doi.org/10.1093/bioinformatics/btv638.

Yang, J., Wang, Y., Zhang, Y., Zeng, X., Liu, J., Tian, Y., Wang, H., Xu, Z., Shen, Y., 2023. Reverse distal similarity of hapten structure enhancing antibody's group-specificity: Development of an immunochromatographic strip for tylosin and tilmicosin in milk and water. J. Food Compos. Anal. 116, 105068. https://doi.org/10.1016/j.jfca.2022.105068.

Yang, J.H., Bhargava, P., McCloskey, D., Mao, N., Palsson, B.O., Collins, J.J., 2017. Antibiotic-Induced changes to the host metabolic environment inhibit drug efficacy and alter immune function. Cell Host Microbe 22, 757–765.e753. https://doi.org/10.1016/j.chom.2017.10.020.

Yopasá-Arenas, A., Fostier, A.H., 2018. Exposure of Brazilian soil and groundwater to pollution by coccidiostats and antimicrobial agents used as growth promoters. Sci. Total Environ. 644, 112–121. https://doi.org/10.1016/j.scitotenv.2018.06.338.

Yuan, J., Hu, Y.J., Zheng, J., Kim, J.H., Sumerlin, T., Chen, Y., He, Y., Zhang, C., Tang, J., Pan, Y., Moore, M., 2020. Long-term use of antibiotics and risk of type 2 diabetes in women: a prospective cohort study. Int. J. Epidemiol. 49, 1572–1581. https://doi.org/10.1093/ije/dyaa122.

Zalewska, M., Błażejewska, A., Czapko, A., Popowska, M., 2021. Antibiotics and antibiotic resistance genes in animal manure–consequences of its application in agriculture. Front. Microbiol. 12, 610656. https://doi.org/10.3389/fmicb.2021.610656.

Zhang, C., Fang, R., Lu, X., Zhang, Y., Yang, M., Su, Y., Jiang, Y., Man, C., 2022. Lactobacillus reuteri J1 prevents obesity by altering the gut microbiota and

regulating bile acid metabolism in obese mice. Food Funct. 13, 6688–6701. https://doi.org/10.1039/D1FO04387K.
Zhang, H., Zhang, Y., Mu, T., Cao, J., Liu, X., Yang, X., Ren, D., Zhao, K., 2023. Response of gut microbiota and ileal transcriptome to inulin intervention in HFD induced obese mice. Int. J. Biol. Macromol. 225, 861–872. https://doi.org/10.1016/j.ijbiomac.2022.11.151.
Zhang, J., Yang, W., Li, S., Yao, S., Qi, P., Yang, Z., Feng, Z., Hou, J., Cai, L., Yang, M., 2016. An intelligentized strategy for endogenous small molecules characterization and quality evaluation of earthworm from two geographic origins by ultra-high performance HILIC/QTOF MS E and progenesis QI. Anal. Bioanal. Chem. 408, 3881–3890. https://doi.org/10.1007/s00216-016-9482-3.
Zhao, F., Gong, Z., Yang, Y., Li, X., Chen, D., Shi, X., Yu, T., Wei, P., 2024. Effects of environmentally relevant concentrations of florfenicol on the glucose metabolism system, intestinal microbiome, and liver metabolome of zebrafish. Sci. Total Environ. 938, 173417. https://doi.org/10.1016/j.scitotenv.2024.173417.
Zhu, Q., Qi, N., Shen, L., Lo, C.C., Xu, M., Duan, Q., Ollberding, N.J., Wu, Z., Hui, D.Y., Tso, P., Liu, M., 2023. Sexual dimorphism in lipid metabolism and gut microbiota in mice fed a high-fat diet. Nutrients 15, 2175. https://doi.org/10.3390/nu15092175.
Zimmermann, P., Curtis, N., 2019. The effect of antibiotics on the composition of the intestinal microbiota - a systematic review. J. Infect. 79, 471–489. https://doi.org/10.1016/j.jinf.2019.10.008.
Zou, M., Cai, Y., Hu, P., Cao, Y., Luo, X., Fan, X., Zhang, B., Wu, X., Jiang, N., Lin, Q., Zhou, H., Xue, Y., Gao, F., 2020. Analysis of the composition and functions of the microbiome in diabetic foot osteomyelitis based on 16S rRNA and metagenome sequencing technology. Diabetes 69, 2423–2439. https://doi.org/10.2337/db20-0503.